Supplementary Information for

Bootstrapping DNA replication with ribonucleotide reductase in a minimal cell-free system

Jacopo De Capitani,[1] Noemi E. Nwosu,[1] Viktoria Gocke,[2] Müge Kasanmascheff,[2] Hannes Mutschler [1*]

Affiliations

1. Biomimetic Chemistry, Department of Chemistry and Chemical Biology, TU Dortmund University, Dortmund, 44227, Germany

2. Physical Chemistry, Department of Chemistry and Chemical Biology, TU Dortmund University, Dortmund, 44227, Germany

*** Corresponding author**: hannes.mutschler@tu-dortmund.de

Table of Contents

Supplementary Methods

PURExpress with FluoroTect™ Green$_{Lys}$ tRNA

Assessment of expression of RNR Ia subunits was carried out in PURExpress (NEB) reactions of 12.5 µL, prepared according to the manufacturer's instructions. RNR Ia synthesis was tested from different expression constructs: pET29b RNR plasmids, pUC19 RNR plasmids or RNR linear constructs. In all cases, the expression cassettes are identical for each RNR subunit. Linear constructs were isolated from pET29b using the Q5 HotStart High-Fidelity 2x Master Mix (NEB) according to the manufacturer's instructions and with primers pr18 and pr19. 4 nM of each RNR Ia construct (both RNR α and β) and 0.6 µL of FluoroTect™ Green$_{Lys}$ tRNA (Promega) were added to the reaction for in vitro translation labeling of de novo expressed RNR Ia subunits. Reactions were then incubated at 37 ºC for 4 hours. Reactions were then treated with 0.6 µL of RNase Cocktail Enzyme Mix (ThermoFisher Scientific) for 15 minutes at 37 ºC to degrade non-incorporated Green$_{Lys}$ tRNA. After treatment, 7.5 µL of each reaction was mixed with an equal volume of 2x Laemmli SDS sample loading buffer and incubated at 65 ºC for 2.5 minutes. Samples were then loaded on a 10% SDS-PAGE gel, which was then imaged in a Sapphire Biomolecular Imager (Azure Biosystems) at 650 nm and 480 nm, to visualize the BlueClassic Prestained Protein Ladder (Jena Bioscience) and the samples respectively. Band volumes from SDS-PAGE were normalized by number of Lys residues in each RNR subunit (42 K in RNR Ia α and 16 K in RNR Ia β). Expression of each subunit was then calculated as a function of the total of de novo protein expression (i.e. sum of normalized band volumes of RNR Ia subunits) (Eq. 1).

$$Expression_{Sub} = \frac{\frac{Band\ Volume_{Sub}}{nLys_{Sub}}}{\left(\frac{Band\ Volume_{\alpha}}{nLys_{\alpha}}\right) + \left(\frac{Band\ Volume_{\beta}}{nLys_{\beta}}\right)} \quad (1)$$

Determination of apparent reaction rate in FLARE assay

The raw RFU data was normalized with min-max scaling between the averages of the t0 of the internal negative controls and the maximum amplitude of positive controls (e.g. ΔRNR, dDTPs - negative; ΔRNR, dNTPs - positive). The normalized RFU data was then smoothened with a Savitzky–Golay filter to reduce noise in the data without distorting data tendency. The filtered data was then fit to a scaled logistic function (Eq. 2) where L is the curve's asymptote, k is the steepness of the curve, x_0 is the midpoint of the logistic function and b is the y-offset of the curve. The second derivative of the fitted logistic function (Eq. 3) was computed to estimate the coordinates of the critical points. The local maximum of the derivative was defined as the end of the lag phase in the reaction signal, while the local minimum was the end of the log phase of exponential fluorescence increase. A linear regression model was then fit to the smoothened data between the x coordinates of the second derivative's critical points. The apparent rate of the reaction is then defined as the slope of the fitted linear model. Lower conversion rates of NDP substrates into dNTPs result in lower transcription rates of the Broccoli RNA aptamer and therefore lower apparent rates in the log phase. An example of apparent rate determination is shown in Supplementary Figure 20.

$$Y = \frac{L}{1 + e^{-k(x - x_0)}} + b \quad (2)$$

$$Y = \frac{k^2 L e^{[k(x-x_0)]}\left(e^{[k(x-x_0)]} - 1\right)}{(1 + e^{[k(x-x_0)]})^3} \quad (3)$$

Expression and purification of *E. coli* RNR 1a α2

Purification of RNR Ia α2 dimer (NrdA) was performed as previously described.[1,2] If not stated otherwise,

50 mM Tris-HCl buffer containing 5% glycerol and 2 mm DTT at pH 7.6 was used for all purification steps, shortly termed *TrisA*. *E. coli* BL21(DE3)-Gold were transformed with pET28a-nrdA and plated on LB-agar plates with 50 μg·mL^{-1} kanamycin (Km) at 37 °C. Isolated colonies were confirmed to contain pET28a-nrdA via Sanger sequencing (Microsynth AG) and used to generate 5 mL LB starter cultures, grown at 37 ºC overnight. The starter cultures were used to inoculate 1 L of LB media (containing Km), which was grown at 37 ºC for 5 hours of overexpression and was induced with 0.5 mm IPTG at OD600 = 0.6 and harvested by centrifugation at 17000 RCF for 15 min at 4 °C. The cell pellet was resuspended in *TrisA* buffer (5 mL·g^{-1} cell pellet), supplemented with 1 mM PMSF and lysed via four passages through an EmulsiFlex-C5 cell homogenizer (Avestin, Inc., Ottawa, ON, Canada). Insoluble cell debris was removed at 3200 RCF for 30 minutes at 4 °C. The DNA was precipitated by adding a 6% (w/v) streptomycin solution (0.2 vol eq.) dropwise, followed by centrifugation at 3200 RCF for 30 minutes at 4 °C. The clear supernatant was loaded onto a Ni-Sepharose High Performance column (Cytiva, Marlborough, MA, USA) pre-equilibrated with *TrisA* buffer containing 20 mM imidazole and 200 mM NaCl. The column was first washed with the same buffer, and the protein was eluted by raising the imidazole concentration to 250 mM. The eluted protein was precipitated by 60% saturation with $(NH_4)_2SO_4$ (2.95 M). The salt was slowly added for over 10 min and stirred for an additional 15 minutes on ice. Then, the protein was isolated at 3200 RCF for 30 min at 4 °C and resolubilized in a minimal amount of *TrisA* buffer. Desalting was performed using a PD-10 column (Sephadex G-25 Medium, Cytiva), pre-equilibrated with *TrisA* buffer. The purified protein was concentrated using an Amicon centrifugal filter unit (30 kDa cutoff, Merck KGaA), and the concentration was determined via UV-Vis spectroscopy with an extinction coefficient at 280 nm of 189,000 M^{-1} cm^{-1}. Aliquots were flash frozen in liquid nitrogen and stored at −80 °C. A typical yield of 2–4 mg protein·g^{-1} cell paste was obtained.

Expression and purification of *E. coli* RNR 1a apo-β2

Purification of RNR Ia apo-β2 dimer (NrdB) was performed as previously described.[1,2] If not stated otherwise, 50 mM Tris-HCl buffer containing 5% glycerol at pH 7.6 was used for all purification steps, shortly termed *TrisB*. *E. coli* BL21(DE3)-Gold were transformed with pTB-nrdB and plated on LB-agar plates with 100 μg·mL^{-1} carbenicillin (Carb) at 37 °C. Isolated colonies were confirmed to contain pTB-nrdB via Sanger sequencing (Microsynth AG) and used to generate 5 mL LB starter cultures, grown at 37 ºC overnight. A 100-fold dilution of the starter cultures were used to inoculate 1 L of LB media (containing Carb), which was treated with 100 μM 1,10-phenanthroline to chelate iron at OD600 = 0.9 and induced with 0.5 mM IPTG after 20 minutes. After 20 h of protein overexpression at 37 ºC, the cells were harvested by centrifugation at 17 000 RCF for 15 minutes at 4 °C. The cell pellet was resuspended in *TrisB* buffer (5 mL·g^{-1} cell pellet) containing 0.5 mM PMSF. The suspension was lysed via four passages through an Emulsiflex-C5 cell homogenizer (Avestin, Inc.). The insoluble cell debris was removed by centrifugation at 3200 relative centrifugal force (RCF) for 30 minutes at 4 °C. The DNA was then precipitated by adding a 6% (w/v) streptomycin solution (0.2 vol eq.) dropwise. This was followed by centrifugation at 3200 RCF for 30 minutes at 4 °C. The NrdB protein was precipitated by reaching 60% saturation with $(NH_4)_2SO_4$ (39 g/100 mL) by slowly adding the salt over 10 minutes and stirring for an additional 15 minutes on ice. The protein was then isolated at 3200 RCF for 30 minutes at 4 °C and resolubilized in a minimal amount of Tris-HCl buffer solution. Desalting was performed using a PD-10 column (Sephadex G-25 Medium, Cytiva) that was pre-equilibrated with Tris-HCl buffer. The protein-containing fractions were then loaded onto anion-exchange column (DEAE Sepharose Fast Flow, Cytiva) pre-equilibrated with *TrisB* buffer supplemented with 100 mM NaCl. Protein elution was carried out with a gradient of 100 to 500 mM NaCl. The protein-containing fractions were pooled and diluted with an equal volume of Tris-HCl buffer to avoid high salt concentrations. The proteins were then purified via a second anion-exchange column (Q Sepharose Fast Flow, Cytiva). The column was equilibrated and washed with *TrisB* buffer supplemented with 150 mM NaCl, and elution was performed with a NaCl gradient from 150 to 500 mM. The protein concentration was determined via UV-Vis spectroscopy. EDTA was then added to the solution at a final concentration 100 times greater than the protein concentration. The solution was then incubated for 2 hours at 4 °C. The EDTA was then removed by washing the solution several times with *TrisB* buffer in a 30-kDa cutoff Amicon centrifugal filter unit (Merck KGaA). After removing the EDTA and reaching the desired protein concentration, the solution was frozen in liquid nitrogen and stored at −80 °C. A typical yield of 9–18 mg protein·g^{-1} cell paste was obtained. For the apoprotein, an extinction coefficient at 280 nm of 120 000 M^{-1} cm^{-1}

was used for concentration determination.

FLARE assay with purified RNR Ia subunits in PURExpress

Purified RNR Ia subunits were used to establish reliability of the FLARE assay read-out in PURExpress reactions independently of RNR Ia expression. In this case, FLARE reactions were prepared as usual (see Supplementary Table 5). Purified RNR Ia apo-β2 was pre-treated with 5 equivalents of ammonium iron(II) sulfate (prepared fresh each time) and left to incubate on ice in an open reaction tube for 10 minutes to ensure Fe^{2+} incorporation and Y_{122}• radical formation. FLARE reactions were then supplemented with 1 μM of each subunit and with 2 mM of one of each NDP (prepared fresh each time), added to the respective reactions. Reactions were then incubated at 30 ºC in a StepOne Real-Time PCR System (ThermoFisher Scientific) for 6 hours (measurement every 6 minutes).

FLARE assay with EDTA titration and Fe^{2+} re-supplementation

To determine if the FLARE assay was capable of confirming the formation of the tyrosyl radical (Y_{122}•) in the de novo synthesized RNR Ia β2 dimer, FLARE reactions without any additional ammonium iron(II) sulfate, were pre-treated with varying concentrations of EDTA (0, 1, 2.5, 5, 10 or 20 μM) to chelate free Fe^{2+} already present in PURExpress and which would contribute to radical formation. After adding EDTA, FLARE reactions were incubated on ice for 10 minutes before incubation at 30 ºC in a StepOne Real-Time PCR System (ThermoFisher Scientific) for 6 hours (measurement every 6 minutes). The calculated apparent rates of the reactions treated with EDTA were then fit to a four-parameter logistic (Hill) function (Eq. 4).

$$Y = \frac{x_{min} + (x_{max} - x_{min})}{1 + \left(\frac{x}{IC50}\right)^{n}} \tag{4}$$

Similarly, to confirm whether radical formation could be rescued after EDTA treatment, FLARE reactions without any additional ammonium iron(II) sulfate, were incubated with 5 μM of EDTA on ice for 10 minutes, before being supplemented with varying concentrations of ammonium iron(II) sulfate (0, 2.5, 5, 10, 15 or 20 μM) and incubated at 30 ºC in a StepOne Real-Time PCR System (ThermoFisher Scientific) for 6 hours (measurement every 6 minutes). The calculated apparent rates of the reactions treated with EDTA and then supplemented with Fe^{2+} where then fit to a four-parameter logistic (Hill) function (Eq. 5).

$$Y = x_{min} + (x_{max} - x_{min})\left(\frac{x^{n}}{EC50^{n} + x^{n}}\right) \tag{5}$$

Site-directed mutagenesis of RNR variants

Construction of RNR Ia variants in pET29b backbones was carried out by site-directed mutagenesis using the Q5 HotStart High-Fidelity 2x Master Mix (NEB) according to the manufacturer's instructions and with the primers specified in Supplementary Table 2. Blunt-end PCR products were then treated and re-ligated with the KLD Mix (NEB) for 1 hour at 25 ºC and then transformed in chemically competent Top10 *E. coli* cells and plated on LB agar plates with 50 μg/mL kanamycin. Clones were grown in liquid LB media with 50 μg/mL kanamycin and plasmid variants were isolated with the NucleoBond Xtra Midi Kit (Machery-Nagel). In the case of RNR Ia β W48 variants, a degenerate primer pair was used, and 6 different variants were isolated. All mutagenized plasmids were confirmed with Sanger sequencing (Microsynth AG).

Preparation of Amino Acid Mix for TTcDR 10x D-EM Mix

The Amino Acid Mix required for the preparation of the 10x D-EM mix for TTcDR PURE reactions (detailed in Supplementary Table 6), was prepared by first dissolving solid amino acid powders (Carl Roth) in 5 M KOH and neutralized with a few drops of glacial acetic acid, for a final concentration of 2 M. Individual amino acids were mixed together with a final concentration of 50 mM. The resulting mixture was neutralized with glacial acetic acid, aliquoted and stored at -80 ºC.

FLARE with TTcDR PURE

The FLARE assay was tested in TTcDR PURE to determine if the optimized composition for TTcDR would improve the assay read-out compared to PURExpress. 17 µL reactions were prepared with 1x D-EM, 0.1x PURExpress Solution A (NEB), 2x PURExpress Solution B (NEB), 1x of TTcDR rNTP Mix, 1 U/µL Murine RNase Inhibitor (NEB), 500 nM ssDNA/prBRO mix, 10 µM DFHBI-1T, 200 µM dDTPs and 1 µL of Phi29 DNAP (NEB) (0.6 U/µL). When FLARE read-out was dependent on purified RNR Ia, RNR Ia β2 was first pre-treated on ice for 10 minutes with 5 equivalents of ammonium iron(II) sulfate (freshly prepared) and then 1 µM of each subunit was supplemented to the FLARE reactions. When FLARE read-out was dependent on de novo expression of RNR Ia, 4 nM of each pET29b RNR plasmid was added to the FLARE reactions. Reactions were then incubated at 30 ºC for 6 hours in a StepOne Real-Time PCR System (ThermoFisher Scientific) (measurement every 6 minutes).

Transformation efficiency of C2C steps

Comparison of transformation efficiencies at individual steps of the circle-to-circle procedure for plasmids replicated in TTcDR PURE was carried out with 3 nM of pET29b RNR Beta plasmid in a TTcDR PURE mixture supplemented with 600 µM dNTP mixture. The steps tested were (1) no restriction enzyme and no ligase, (2) no restriction enzyme, but ligase, and (3) restriction enzyme and ligase. The TTcDR reactions were incubated at 30 ºC for 16 hours and subsequently treated with 60 U (3 µL) of DpnI (NEB) for 3 hours at 37 ºC. Reactions 2 and 3 were incubated with 50 U (1 µL) of ApaI (NEB) for 1 hour at 37 ºC. Reaction 3 was then supplemented with ATP to a final concentration of 1 mM and 800 U (2 µL) of Salt-T4 Ligase (NEB) and incubated at 25 ºC for 16 hours. 1 µL of 1:10 dilution of each complete reaction was then transformed in chemically competent Top10 cells and plated on LB agar plates with 50 µg/mL kanamycin.

Supplementary Tables

DNA sequences

Supplementary Table 1: Primers used in cloning RNR plasmids.

Primer Number / Oligo Name	Sequence
pr01 (RNR Ia locus cloning in pBAD33 - FWD)	ATGAGAGGATCGCATCACCATCACCATCACGGATCCA ATCAGAATCTGCTGGTG
pr02 (RNR Ia locus cloning in pBAD33 - REV)	CAGCCAAGCTTCGTAAATTCTATACAAAATCAGAGCT GGAAGTTACT
pr03 (pBAD33 backbone - FWD)	TTTTGTATAGAATTTACGAAGCTTGGCTGT
pr04 (pBAD33 backbone - REV)	GGATCCGTGATGGTGATGGTGATGCGATCCTCTCAT
pr05 (RNR Ia locus cloning in pET29b with pBAD33 RBS - FWD)	AGCGGATAACAATTCCCCTCTAGAAATAATTTAACTT TAAGAAGGAGATATACC
pr06 (RNR Ia locus cloning in pET29b with pBAD33 RBS - REV)	TTCCTTTCGGGCTTTGTTAGCAGCCGGATCTCAGAGC TGGAAGTTACTC
pr07 (pET29b backbone - FWD)	GATCCGGCTGCTAACAAA
pr08 (pET29b backbone - REV)	ATTATTTCTAGAGGGGAATTGTTATC
pr09 (pET29b RNR Alpha 6xHis - FWD)	GATCCGGCTGCTAACAAAGCCCGAAAGGAA
pr10 (pET29b RNR Alpha 6xHis - REV)	CCGCATCCGGCATCTCAATATCAGATCTTACATGC
pr11 (pET29b RNR Beta - FWD)	ACGAAAAATGATCAGCTCAAAGAACCGATGTT
pr12 (pET29b RNR Beta - REV)	CTGTGAAAAGGTGGTATATGCCATGGTATATCTCCTT CTTAAAG
pr13 (pUC19 RNR - FWD)	GGGTGTTGGCGGGTGTCGGGGCTGGCTTAATCGATCC CGCGAAATTAATAC
pr14 (pUC19 RNR - REV)	GCGGATAACAATTTCACACAGGAAACAGCTCAAAAA ACCCCTCAAGACCC
pr15 (pUC19 backbone - FWD)	AGCTGTTTCCTGTGTGAAATTG
pr16 (pUC19 backbone - REV)	TTAAGCCAGCCCCGA
pr17 (RNR expression cassette - FWD)	GATCCCGCGAAATTAATACGACTC
pr18 (RNR expression cassette - REV)	AGTTCCTCCTTTCAGCAAAAAAC

Supplementary Table 2: Primers used for site-directed mutagenesis of RNR Ia subunits. Mutated codon is underlined.

Primer Number / Oligo Name	Sequence
pr19 (RNR Ia β W48 - FWD)	NNNCGTCCGGAAGAAGTTG
pr20 (RNR Ia β W48 - REV)	GAAGAAAGAGAGCTGC
pr21 (RNR Ia β E52L - FWD)	GCGTCCGGAACTGGTTGACGTCTC
pr22 (RNR Ia β E52L - REV)	CAGAAGAAAGAGAGCTG
pr23 (RNR Ia α R411A - FWD)	GTCTACCGGTGCGATCTATATTCAGAACG
pr24 (RNR Ia α R411E - FWD)	GTCTACCGGTGAAATCTATATTCAGAAC
pr25 (RNR Ia α R411L - FWD)	GTCTACCGGTCTGATCTATATTCAG
pr26 (RNR Ia α R411Q - FWD)	GTCTACCGGTCAGATCTATATTCAG
pr27 (RNR Ia α R411 - REV)	GCACGTTCCTGCATC

Supplementary Table 3: Coding sequences of proteins used in this study.

Coding Sequence	Sequence
RNR 1a Alpha (6xHis) (*nrdA*)	atgagaggatcgcatcaccatcaccatcacggatccaatcagaatctgctggtgacaaagcgcgacggtagcacagagcg catcaatctcgacaaaatccatcgcgttctggattgggcggcagaaggactgcataacgtttcgatttcccaggtcgagc tgcgctcccacattcagttttatgacggtatcaagacctctgacatccacgaaaccattatcaaggctgccgcagacctg atctcccgtgatgcgccggattatcagtatctcgccgcgcgcctggcgatcttccacctgcgtaaaaaagcctacggcca gtttgagccgcctgcgctgtacgaccacgtggtgaaaatggtcgagatgggcaaatacgataatcatctgctggaagact acacggaagaagagttcaagcagatggacacctttatcgatcacgaccgtgatatgaccttctcttatgctgccgttaag cagctggaaggcaaatatctggtacagaaccgcgtgaccggcgaaatctatgagagcgcccagttcctttatattctagt tgccgcgtgcttgttctcgaactacccgcgtgaaacgcgcctgcaatatgtgaagcgtttttacgacgcggtttccacat ttaaaatttcgctgccgacgccaatcatgtccggcgtgcgtaccccgactcgtcagttcagctcctgcgtactgatcgag tgcggtgacagcctggattccatcaacgccacctccagcgcgattgttaaatacgtttcccagcgtgccgggatcggcat caacgccgggcgtattcgtgcgctgggtagcccgattcgcggtggtgaagcgttccataccggctgcattccgttctaca aacatttccagacagcggtgaaatcctgctctcagggcggtgtgcgcggcggtgcggcaacgctgttctacccgatgtgg catctggaagtggaaagcctgctggtgttgaaaaacaaccgtggtgtggaaggcaaccgcgtgcgtcatatggactacgg ggtacaaatcaacaaactgatgtatacccgtctgctgaaaggtgaagatatcaccctgttcagcccgtccgacgtaccgg ggctgtacgacgcgttcttcgccgatcaggaagagtttgaacgtctgtataccaaatatgagaaagacgacagcatccgc aagcagcgtgtgaaagccgttgagctgttctcgctgatgatgcaggaacgtgcgtctaccggtcgtatctatattcagaa cgttgaccactgcaatacccatagcccgtttgatccggccatcgcgccagtgcgtcagtctaacctgtgcctggagatag ccctgccgaccaaaccgctgaacgacgtcaacgacgagaacggtgaaatcgcgctgtgtacgctgtctgctttcaacctg ggcgcaattaataacctggatgaactggaagagctggcaattctggcggttcgtgcacttgacgcgctgctggattatca ggattacccgatcccggccgccaaacgtggagcgatgggtcgtcgtacgctgggtattggtgtgatcaacttcgcttact acctggcgaagcacggtaaacgctactccgacggcagcgccaacaacctgacgcataaaaccttcgaagccattcagtat tacctgctgaaagcctctaatgagctggcgaaagagcaaggcgcgtgcccgtggtttaacgaaaccacttacgcgaaagg gatcctgccgatcgatacctataagaaagatctggataccatcgctaatgagccgctgcattacgactgggaagctctgc gtgagtcaatcaaaacgcacggtctgcgtaactccacgctttctgctctgatgccgtccgagacttcttcgcagatctct aacgccactaacggtattgaaccgccgcgcggttacgtcagcatcaaagcgtcgaaagacggtattttgcgccaggtggt gccggactacgagcacctgcacgacgcctatgagctgctgtgggaaatgccgggtaacgatggttatctgcaactggtgg gtatcatgcagaaatttatcgatcagtcgatctctgccaacaccaactacgatccgtcacgcttcccgtcaggaaaagtg ccgatgcagcagttgctgaaagacctgctcaccgcctacaaattcggggtcaaaacactgtattatcagaacacccgtga cggcgctgaagacgcacaagacgatctggtgccgtcaatccaggacgatggctgcgaaagcggcgcatgtaagatctga
RNR 1a Beta (*nrdB*)	atggcatataccacctttttcacagacgaaaaatgatcagctcaaagaaccgatgttctttggtcagccggtcaacgtggc tcgctacgatcagcaaaaatatgacatcttcgaaaagctgatcgaaaagcagctctctttcttctggcgtccggaagaag ttgacgtctcccgcgaccgtatagattaccaggcgctgccggagcacgaaaaacacatctttatcagcaacctgaaatat cagacgctgctggattccattcagggtcgtagcccgaacgtggcgctattgccgcttatttctattccggaactggaaac ctgggtcgaaacctgggcgttctcagaaacgattcattcccgttcctatactcatatcattcgtaatatcgttaacgatc cgtctgttgtgtttgacgatatcgtcaccaacgagcagatccagaaacgtgcggaagggatctccagctattacgatgag ctgatcgaaatgaccagctactggcatctgctgggcgaaggtacccacaccgttaacggtaaaactgtgaccgttagcct

	gcgcgagctgaagaaaaaactgtatctctgcctgatgagcgttaacgcgctggaagcgattcgtttctacgtcagctttg cttgttccttcgcatttgcagaacgcgaattgatggaaggcaacgccaaaattattcgcctgattgcccgcgacgaagcc ctgcacctgaccggcacccagcatatgctgaatctgctgcgcagcggcgcggacgatcctgagatggcggaaattgccga agagtgtaagcaggagtgctatgacctgtttgttcaggcagctcaacaggagaaagactgggcggattatctgttccgcg acggttcgatgattggtctgaataaagacattctctgccagtacgttgaatacatcaccaatatccgtatgcaggcagtc ggtttggatctgccgttccagacgcgctccaacccgatcccgtggatcaacacttggctggtgtctgataacgtgcaggt tgctccgcaggaagtggaagtcagttcttatctggtcgggcagattgactcggaagtggacaccgacgatttgagtaact tccagctctga
Phi29 DNA polymerase	atgccgagaaagatgtatagttgtgactttgagacaactactaaagtggaagactgtagggtatgggcgtatggttatat gaatatagaagatcacagtgagtacaaaataggtaatagcctggatgagtttatggcgtgggtgttgaaggtacaagctg atctatatttccataacctcaaatttgacggagcttttatcattaactggttggaacgtaatggttttaagtggtcggct gacggattgccaaacacatataatacgatcatatctcgcatgggacaatggtacatgattgatatatgtttaggctacaa agggaaacgtaagatacatacagtgatatatgacagcttaaagaaactaccgtttcctgttaagaagatagctaaagact ttaaactaactgttcttaaaggtgatattgattaccacaaagaaagaccagtcggctataagataacacccgaagaatac gcctatattaaaaacgatattcagattattgcggaagctctgttaattcagtttaagcaaggtttagaccggatgacagc aggcagtgacagtctaaaaggtttcaaggatattataaccactaagaaattcaaaaaggtgtttcctacattgagtcttg gactcgataaggaagtgagatacgcctatagaggtggttttacatggttaaatgataggttcaaagaaaaagaaatcgga gaaggcatggtcttcgatgttaatagtctatatcctgcacagatgtatagccgtctccttccatatggtgaacctatagt attcgagggtaaatacgtttgggacgaagattacccactacacatacagcatatcagatgtgagttcgaattgaaagagg gctatatacccactatacagataaaaagaagtaggttttataaaggtaatgagtacctaaaaagtagcggcggggagata gccgacctctggttgtcaaatgtagacctagaattaatgaaagaacactacgatttatataacgttgaatatatcagcgg cttaaaatttaaagcaactacaggtttgtttaaagattttatagataaatggacgtacatcaagacgacatcagaaggag cgatcaagcaactagcaaaactgatgttaaacagtctatacggtaaattcgctagtaaccctgatgttacagggaaagtc ccttatttaaaagagaatggggcgctaggtttcagacttggagaagaggaaacaaaagaccctgtttatacacctatggg cgttttcatcactgcatgggctagatacacgacaattacagcggcacaggcttgttatgatcggataatatactgtgata ctgacagcatacatttaacgggtacagagatacctgatgtaataaaagatatagttgaccctaagaaattgggatactgg gcacatgaaagtacattcaaaagagctaaatatctgagacagaagacctatatacaagacatctatatgaaagaagtaga tggtaagttagtagaaggtagtccagatgattacactgatataaaatttagtgttaaatgtgcgggaatgactgacaaga ttaagaaagaggttacgtttgagaatttcaaagtcggattcagtcggaaaatgaagcctaagcctgtgcaagtgccgggc ggggtggttctggttgatgacacattcacaatcaaataa

Supplementary Table 4: Oligos for FLARE assay.

Primer Number / Oligo Name	Sequence
Broccoli ssDNA	GAAATTAATACGACTCACTATAGGGAGACGGTCGGGTCCA GATATTCGTATCTGTCGAGTAGAGTGTGGGCTCCC
prBRO (REV Broccoli)	GGGAGCCCACACTCTACT

Composition of FLARE assay in PURE

Supplementary Table 5: FLARE assay reaction composition in PURExpress.

Example composition with CDP and dDTP Mix. Concentrations also apply to other NDPs and dNTPs mixes. 17 µL final reaction volume.

Component	Stock Concentration	Final Concentration
PURExpress Solution A (NEB)	2.5x	1x
PURExpress Solution B (NEB)	3.33x	1x
Murine RNase Inhibitor (NEB)	40 U/µL	1 U/µL
ssDNA Broccoli + prBRO Mix	10 µM	0.5 µM
CDP	200 mM	2 mM
dDTPs (equimolar mix dA, dG, dT)	10 mM	0.2 mM
TCEP (Biotium)	200 mM	1.5 mM
Ammonium Iron(II) Sulfate (Carl Roth)	100 µM	5 µM
pET29b RNR Alpha 6x His	150 nM	4 nM
pET29b RNR Beta	150 nM	4 nM
Phi29 DNA Polymerase (NEB)	10 U/µL	0.6 U/µL
DFHBI-1T (Biomol)	1.5 mM	0.01 mM

Composition of TTcDR reactions

Supplementary Table 6: Concentrations of components in 10x D-EM mix for TTcDR reactions.

Component	Stock Concentration	Concentration in Mix
Amino Acid Mix (Carl Roth)	50 mM	3.6 mM
Potassium Glutamate (Sigma)	3.4 M	700 mM
Spermidine (Sigma)	1 M	3.75 mM
Creatine Phosphate (Sigma)	2 M	250 mM
E. coli tRNA (Roche)	38 mg/mL	5.18 mg/mL
HEPES-KOH (Carl Roth)	2.5 M	1 M
Magnesium Acetate (ChemPur)	2 M	79 mM
TCEP (Biotium)	1 M	15 mM

Supplementary Table 7: Concentrations of NTPs in rNTP Mix for TTcDR reactions.

The rNTP Mix is prepared in a 50x stock. 0.25 µL of rNTP Mix is added to each 12.5 µL TTcDR reaction.

NTP	Stock Concentration	Concentration in Mix	Concentration in TTcDR Reaction
ATP	100 mM	18.75 mM	0.375 mM
GTP	100 mM	12.5 mM	0.250 mM
CTP	100 mM	6.25 mM	0.125 mM
UTP	100 mM	6.25 mM	0.125 mM

Supplementary Table 8: TTcDR reaction composition for RNR-dependent plasmid replication.

Example composition with dDTP Mix. Concentrations also apply to other dNTPs mixes. 12.5 µL final reaction volume.

Component	Stock Concentration	Final Concentration
10x D-EM	10x	1x
PURExpress Solution A (NEB)	2.5x	0.1x
PURExpress Solution B (NEB)	3.33x	2x
TTcDR rNTP Mix	50x	1x
Murine RNase Inhibitor (NEB)	40 U/µL	1 U/µL
Ammonium Iron(II) Sulfate (Carl Roth)	500 µM	5 µM
TCEP (Biotium)	200 mM	1.5 mM
pUC19 RNR Alpha 6x His	100 nM	3 nM
pUC19 RNR Beta	100 nM	3 nM
dDTPs (equimolar mix dA, dG, dT)	25 mM	0.6 mM
Phi29 DNA Polymerase (NEB)	10 U/µL	0.8 U/µL

Supplementary Figures

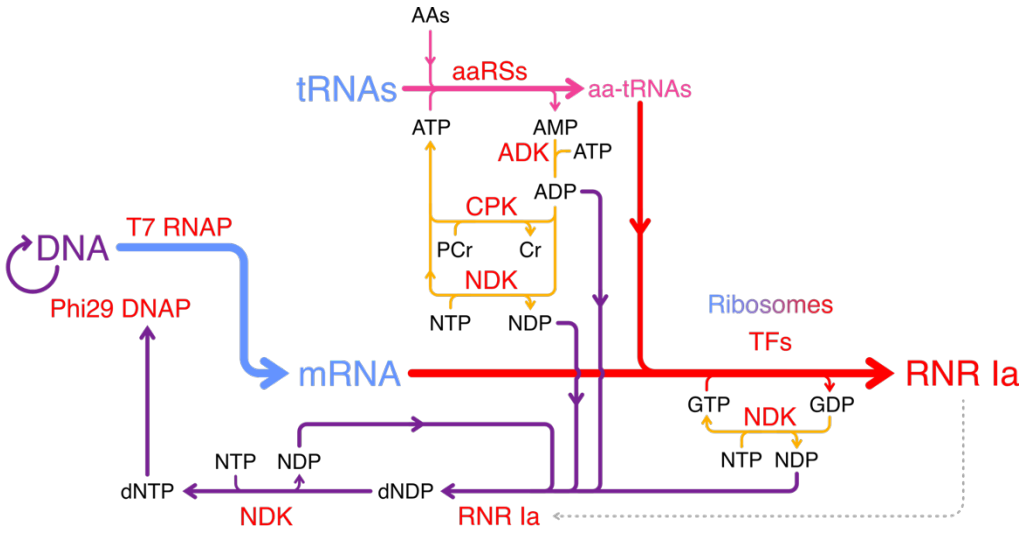

Supplementary Figure 1: PURE metabolic network with integration of dNTP synthesis by RNR Ia.

Schematic of PURE metabolic network showing transcription (blue), translation (red), tRNA aminoacylation (pink) and NTP regeneration (yellow). The standard reaction framework of PURE has been updated to incorporate RNR-mediated synthesis of dNTPs for DNA replication (purple). In this setup, the genes that encode each RNR Ia subunit are located in the input plasmids. These plasmids are then transcribed and translated to produce the functional RNR Ia heterodimer tetrameric complex. RNR Ia then reduces the NDPs produced by nucleoside diphosphate kinase (NDK) and adenylate kinase (ADK) as part of NTP energy regeneration after tRNA aminoacylation and peptide bond formation. NDK then re-phosphorylates the synthesized dNDPs to dNTPs using NTPs as phosphate donors. These dNTPs can then be used by Phi29 to replicate the starting RNR-encoding plasmids.

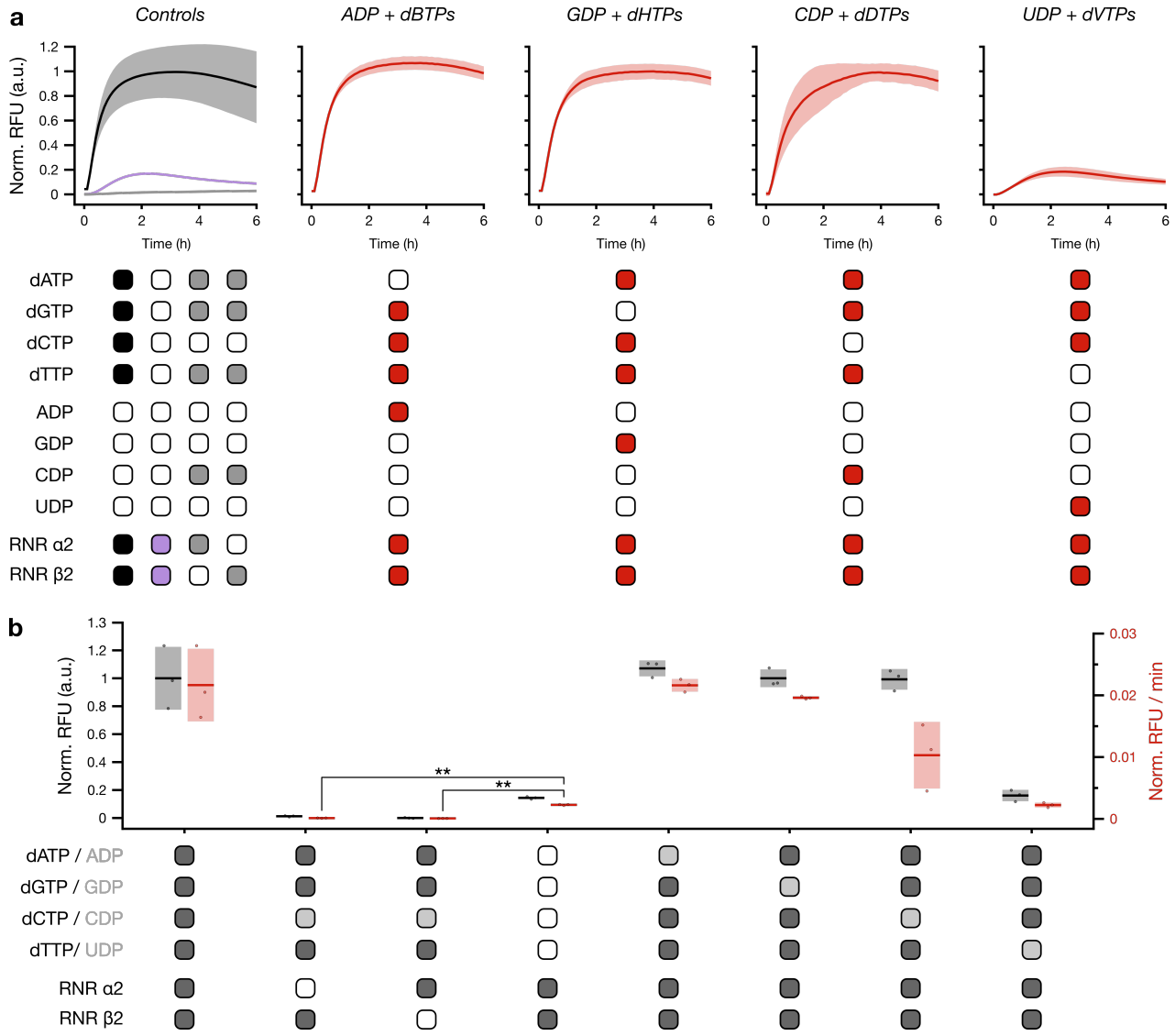

Supplementary Figure 2: FLARE assay in PURExpress with purified RNR Ia subunits.

Characterization of FLARE activity in PURExpress with 1 µM of each RNR Ia subunit. RNR Ia β2 was pre-incubated on ice for 10 minutes with 5 equivalents of ammonium iron(II) sulfate to ensure formation of Y_{122}• radical. Reactions were carried out with additional 2 mM of each NDP missing from the respective dNTP mix (e.g. CDP + dDTPs) In the sample matrices, colored boxes indicate components supplied to the reactions. **a.** Real-time normalized RFU values of FLARE assays dependent on reduction of different NDPs. In the sample matrix, colored boxes indicate components supplied to the reactions. **b.** Maximum normalized RFU measurements (black) and respective apparent reaction rates (red) for different individual NDPs and remaining dNTPs supplied to assay reaction. In the sample matrix, dNTPs supplied to the reactions are marked in dark gray, while NDPs in gray. In reactions where no exogenous NDPs were introduced in PURExpress (i.e. ΔNDPs and ΔdNTPs), RNR-dependent reduction of NDPs generated in PURE resulted in an increase in FLARE read-outs, compared to the samples lacking either RNR subunit (compared to Δα p=0.0021; compared to Δβ p=0.0012). The data was normalized with min-max scaling between max value of dNTPs sample and t0 of Δβ2-dDTPs sample. Technical replicates were performed for all measurements, with n = 3. The mean and standard deviation are shown. Unpaired two-tailed Welch's t-tests were used for pairwise comparisons between the different reaction rates out and corrected for multiple comparisons with FDR.

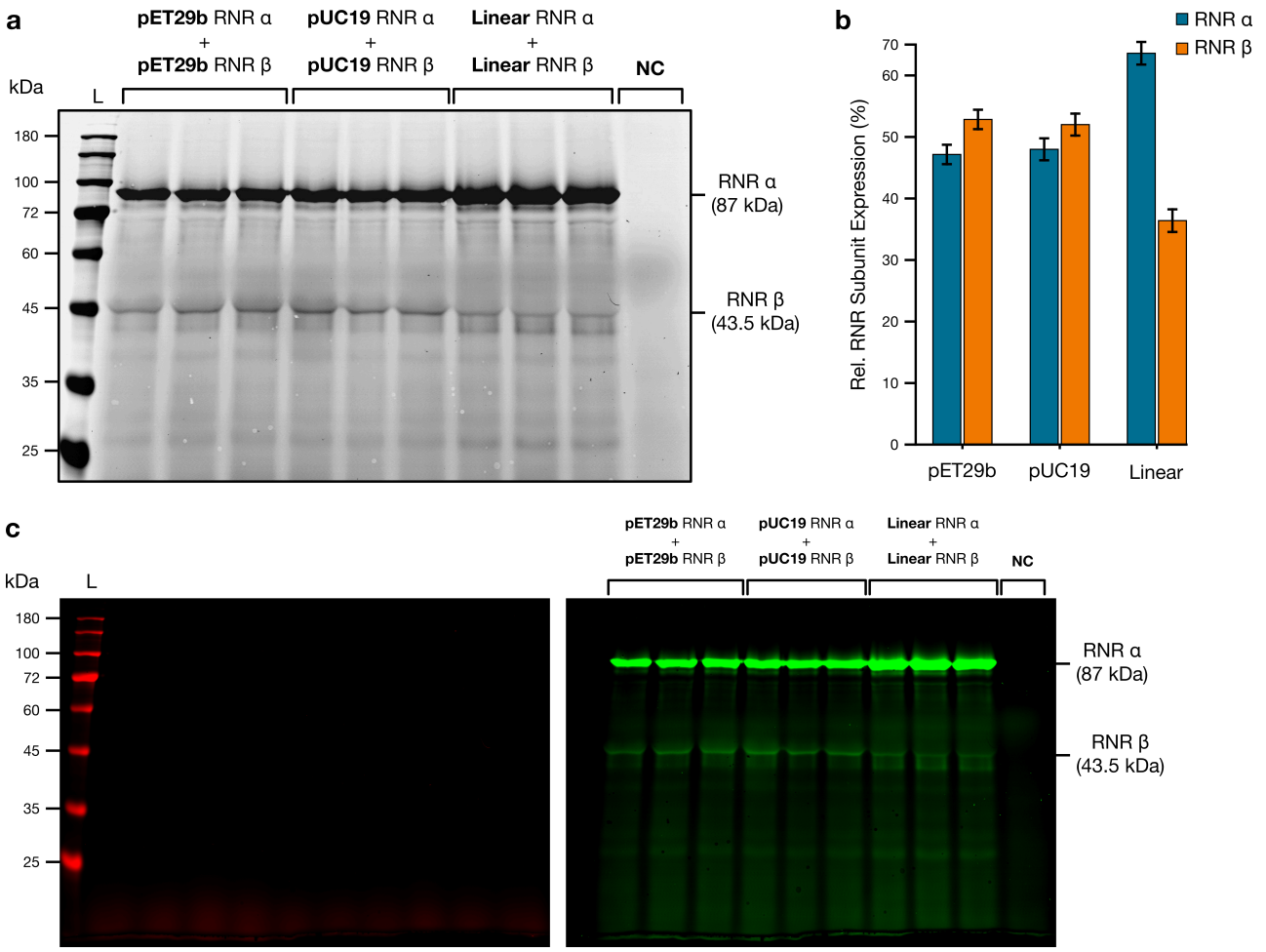

Supplementary Figure 3: Confirmation of RNR subunits expression with PURE supplemented with FluoroTect^{TM} Green$_{Lys}$-tRNA.

a. 10% SDS-PAGE of PURExpress (NEB) reactions supplemented with Green$_{Lys}$-tRNA to confirm expression of each RNR Ia subunit. Gel imaged at 488 nm and 650 nm to visualize samples and BlueClassic Pre-Stained Ladder (Jena Bioscience) respectively. **b.** Expression of each RNR subunit presented as a function of total de novo RNR Ia expression, after normalization of band intensity by number of Lys residues in each subunit. **c.** Uncropped original images of SDS-PAGE gel shown in A. Left - 650 nm excitation for BlueClassic Pre-Stained Ladder. Right - 488 nm excitation for visualization of BODIPY group on Lys residues. Independent replicates were performed for all measurements, with n = 3. The mean and standard deviation are shown.

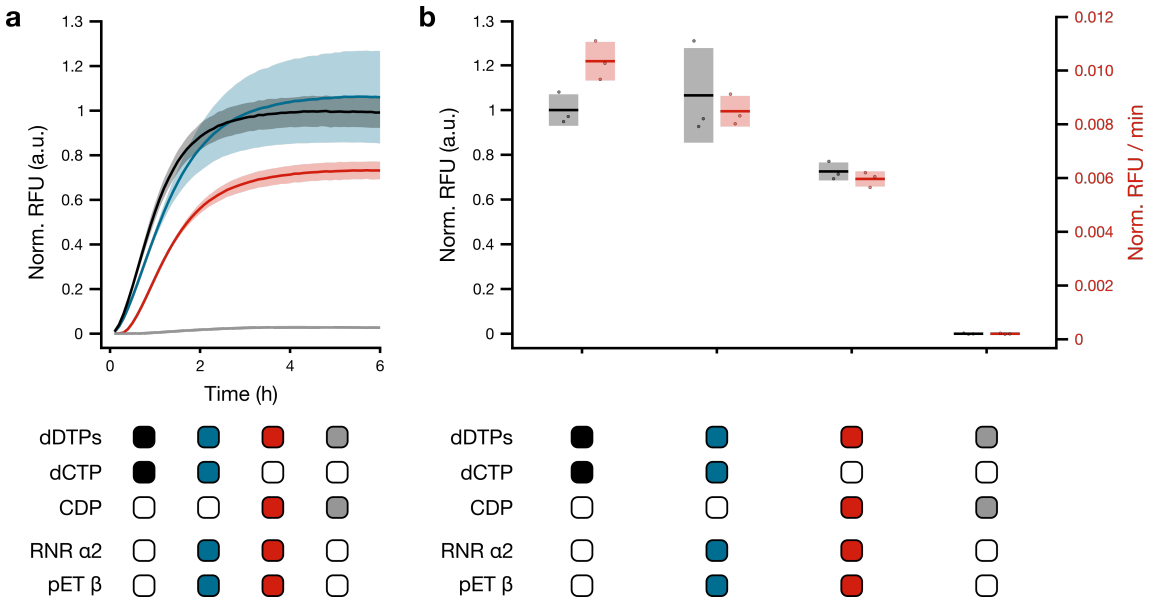

Supplementary Figure 4: FLARE assay in PURExpress with de novo expression of RNR Ia β2 subunit.

Proof-of-concept of FLARE read-out dependent on de novo expression of RNR Ia β2 homodimer and reduction of 2 mM CDP supplemented to PURExpress. In the sample matrices, colored boxes indicate components supplied to the reactions. **a.** Real-time normalized RFU values of FLARE. RNR-independent reactions with all dNTPs supplied, either in the presence (blue) or not (black) of RNR Ia, are compared with reactions dependent on RNR reduction of CDP by RNR Ia with de novo expression of β2 homodimer (red). **b.** Maximum normalized RFU measurements (black) and respective apparent reaction rates (red) for different combinations of dDTPs and CDP supplied to the reaction with RNR Ia β2 expression. The data was normalized with min-max scaling between max value of ΔRNR-dNTPs sample and t0 of ΔRNR-dDTPs sample. Technical replicates were performed for all measurements, with n = 3. The mean and standard deviation are shown.

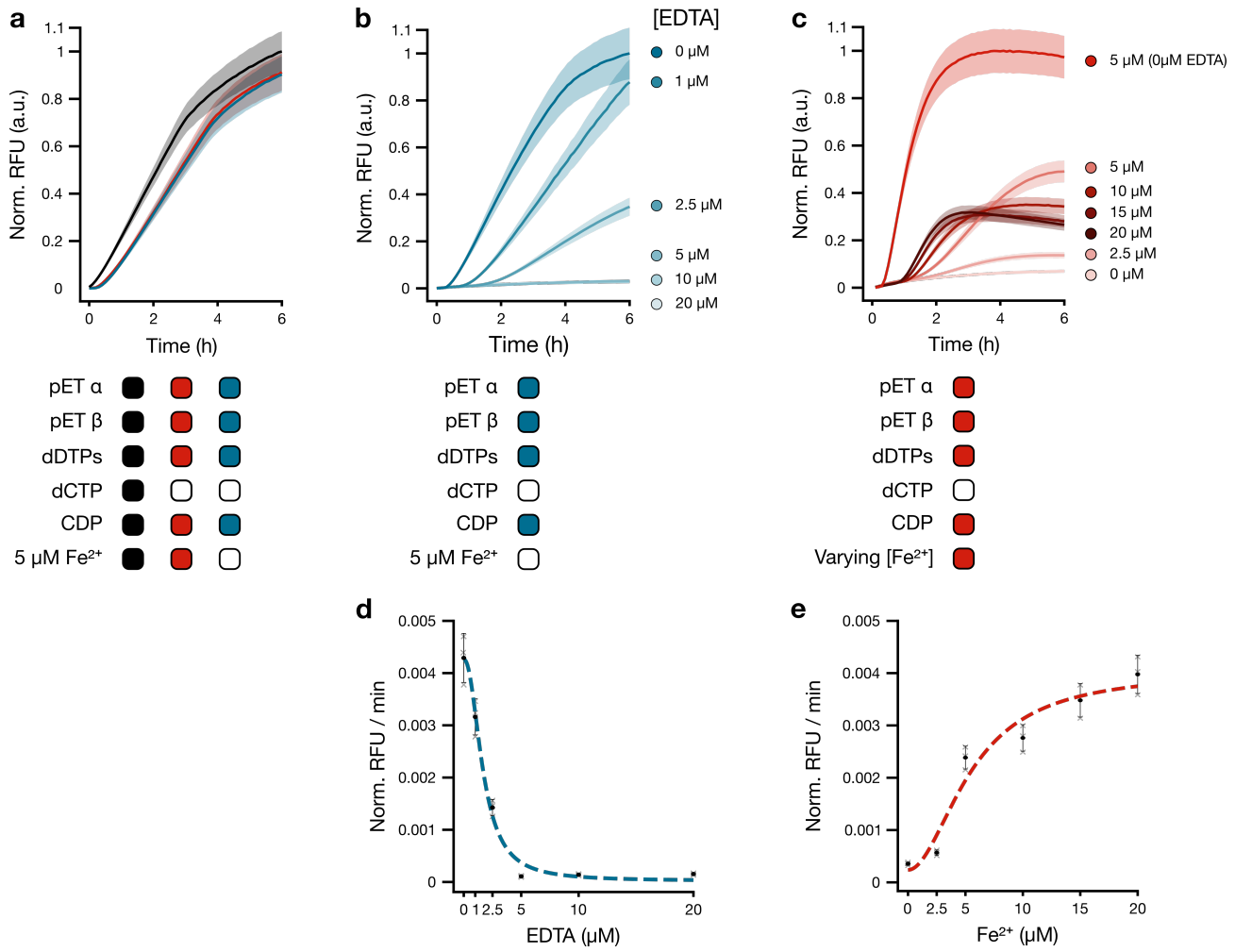

Supplementary Figure 5: Confirmation of Tyr_{122} radical formation in de novo expressed RNR Ia β2.

FLARE assay reactions for the characterization of Y_{122}• radical formation in de novo expressed RNR Ia. Fe^{2+} incorporation is necessary for radical formation and correct β2 folding. Fe^{2+} incorporation and formation of radical can be monitored with FLARE by depleting and re-introducing Fe^{2+} in PURExpress. In the sample matrices, colored boxes indicate components supplied to the reactions. **a.** Normalized real-time RFU measurements of comparison of dCTP synthesis with FLARE with either 5 µM Fe^{2+} or no additional Fe^{2+} added to PURE. The data was normalized with min-max scaling between max value of the dNTPs + 5 µM Fe^{2+} sample and t0 of the same sample. **b.** Detection of RNR-dependent dCTP synthesis after 10 minutes treatment of PURExpress with increasing concentrations of EDTA pre-treatment (0-20 µM) and no additional Fe^{2+} added. The data was normalized with min-max scaling between max value and t0 of the dDTPs sample with no EDTA. **c.** Partial recovery of RNR Ia activity upon re-supplementation of Fe^{2+} (0-20 µM) after treatment of PURExpress with 5 µM of EDTA. FLARE signals did not reach the same maximum fluorescence amplitudes as in the untreated sample likely due chelation by EDTA of other ions important for translation (e.g. zinc for ribosomes). The data was normalized with min-max scaling between max value of the dDTPs + 5 µM Fe^{2+} + 0 µM EDTA sample and t0 of the same sample. **d.** Apparent rates of reactions in panel b, fit to a decay four-parameter logistic function. Estimated IC50 ≅ 2 µM EDTA. **e.** Apparent rates of reactions in panel c, fit to an activation four-parameter logistic function. Estimated EC50 ≅ 5 µM Fe^{2+}. Chelation and re-supplementation of Fe^{2+} confirmed that FLARE signals depended on correctly establishing the di-ferric center and Fe^{3+}-Y_{122}• radical the β subunits of de novo RNR Ia. Technical replicates were performed for all measurements, with n = 3. The mean and standard deviation are shown.

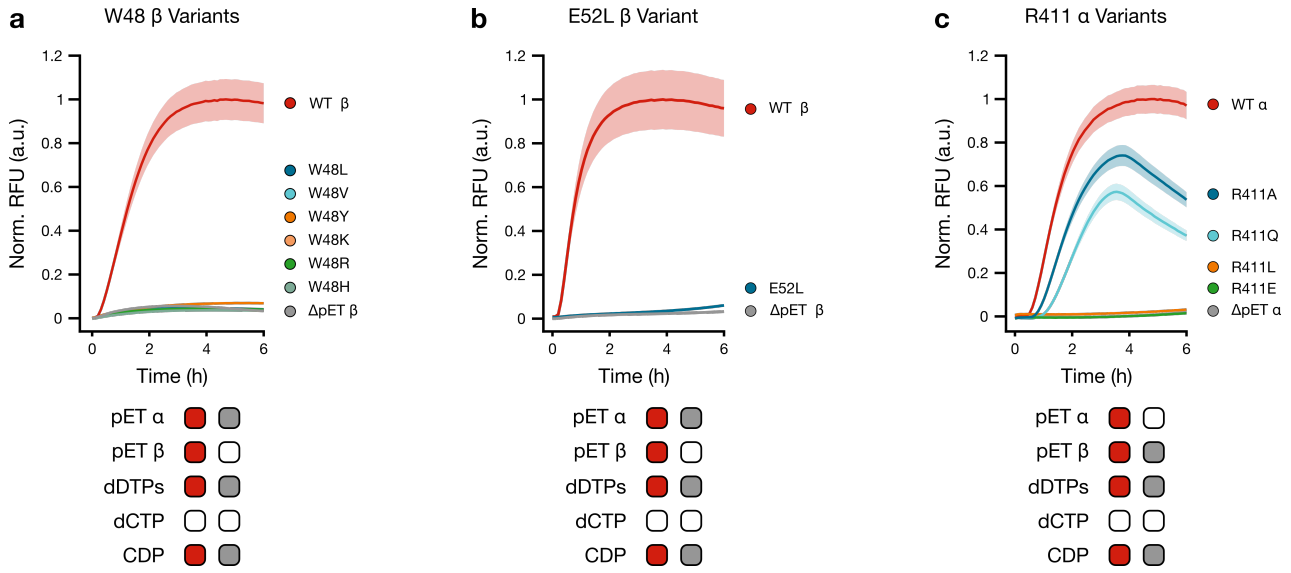

Supplementary Figure 6: Activity of de novo RNR Ia variants with FLARE assay.

The expression of active RNR Ia de novo in PURE depends on its ability to establish the proton-coupled electron transfer (PCET) between the β and α subunits after generation of Y_{122}• radical in each β subunit. The FLARE assay was used to compare RNR-dependent dCTP synthesis between WT RNR Ia and variants of RNR Ia with mutated residues key to PCET. In the sample matrices, red boxes indicate components supplied to the reactions testing different RNR Ia subunit variants. All reactions for testing of variants are supplemented with dDTPs and require reduction of endogenous CDP upon expression of the relative RNR Ia subunit. Gray boxes represent the negative controls lacking the relative subunit being tested. **a.** W48 variants (W48L, W48V, W48Y, W48K, W48R, W48H) of RNR Ia β subunit were tested to determine impairment of PCET.[3] **b.** E52L variant of RNR Ia β subunit is tested to determine effect on mutating key residue in subunit interface between α2 and β2 homodimers.[4,5] **c.** R411 variants (R411A, R411Q, R411L, R411E) of RNR Ia α subunit to determine effect on key residue in PCET at α2β2 interface.[6] Detection of impairment of the PCET (proton-coupled electron transfer) pathway from the β2 to α2 homodimers is shown by mutating the W48 and E52 residues. As previously reported, mutations of the R411 residue at the subunit interface of the RNR Ia complex showed residual activity for the R411A[6] and R411Q[7] variants. The data was normalized with min-max scaling between max value of the respective WT-dDTPs sample and t0 of the respective ΔpET-dDTPs sample of the subunit being investigated. Technical replicates were performed for all measurements, with n = 3. The mean and standard deviation are shown.

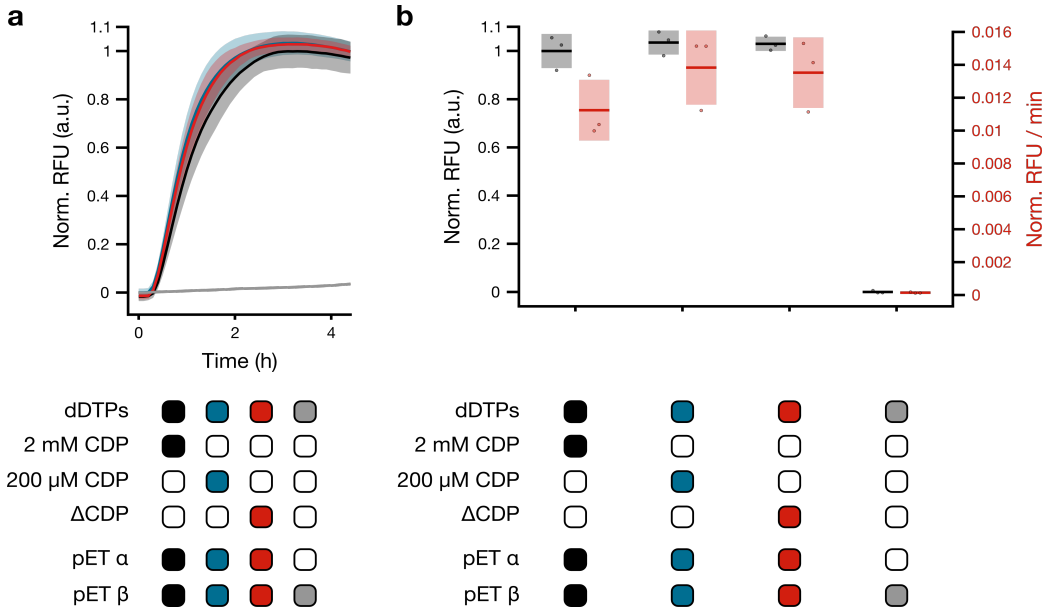

Supplementary Figure 7: FLARE assay with titration of supplemented CDP.

Comparing FLARE read-out by de novo expressed RNR Ia with CDP either supplemented to PURExpress or endogenously produced in PURE. In the sample matrices, colored boxes indicate components supplied to the reactions. dCTP-limiting FLARE reactions (i.e. signal dependent on the reduction of CDP) were used to compare 2 mM CDP supplemented to PURExpress (black boxes) with 200 µM supplemented CDP blue boxes) and with no supplemented CDP (red boxes). The negative control, lacking plasmid for α2 expression, is identified by gray boxes **a.** Real-time normalized RFU values of FLARE titration of CDP supplied to reactions. **b.** Maximum normalized RFU measurements (black) and respective apparent reaction rates (red) for different concentrations of CDP supplied to the reaction. Similar maximum fluorescence values and read-out rates were observed irrespective of CDP input. The data was normalized with min-max scaling between max value of the sample with dDTPs + 2 mM CDP and t0 of the ΔpETα-dDTPs sample. Technical replicates were performed for all measurements, with n = 3. The mean and standard deviation are shown.

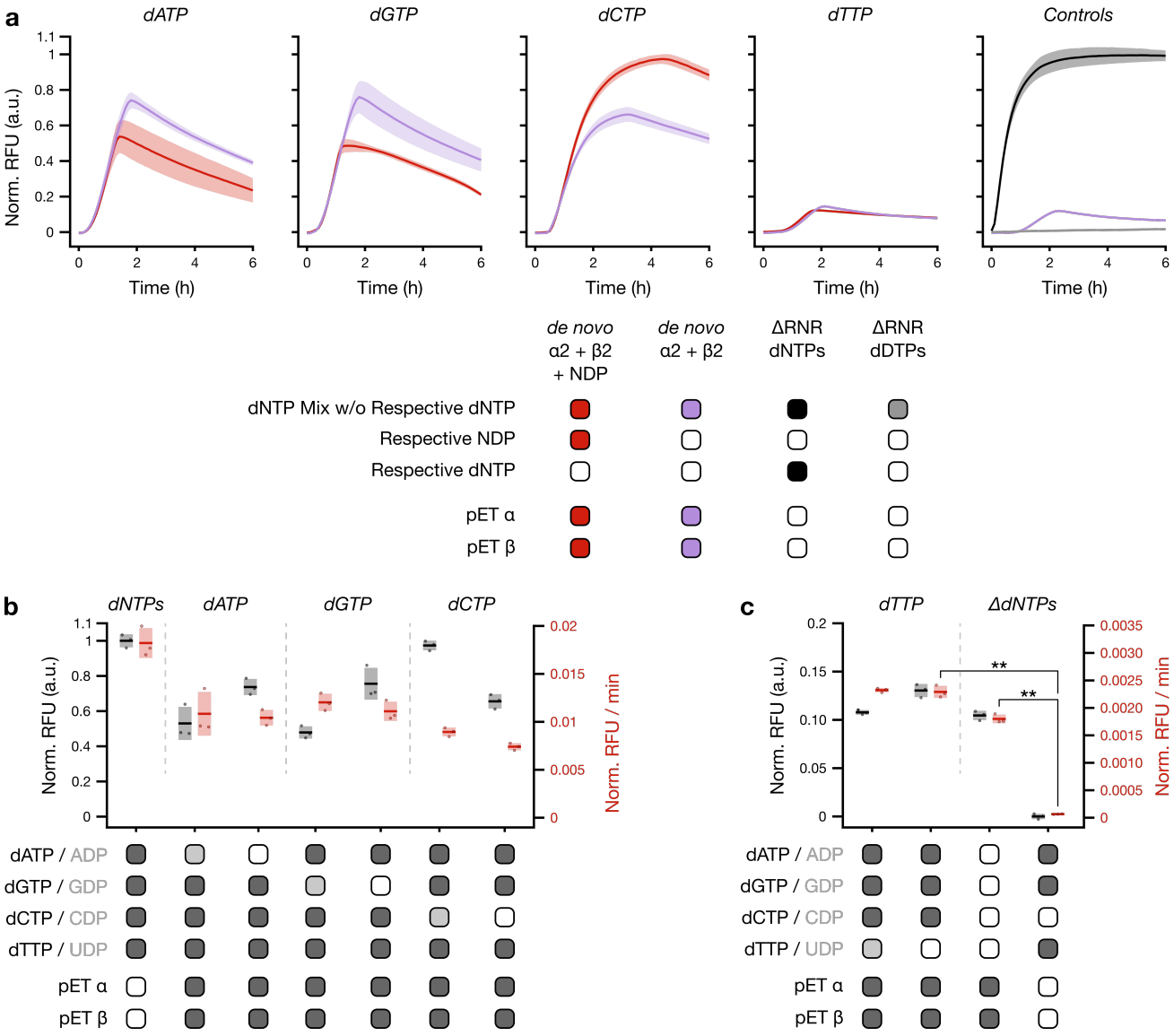

Supplementary Figure 8: Reduction of individual NDPs, either supplied or endogenous to PURE.

FLARE characterization of reduction of individual NDPs by de novo expressed RNR Ia, tested with both externally supplied NDPs and with NDPs endogenously generated in PURE. In the sample matrices, colored boxes indicate components supplied to the reactions. In the matrices in panels b and c, shaded boxes indicate respective NDP supplied externally to PURE.**a.** Normalized real-time RFU measurements of RNR-dependent reduction of individual NDPs either supplied (red) or endogenous to PURE (purple) were compared with reactions without RNR Ia plasmids with either all dNTPs (black – positive control) or only dDTPs (gray – negative control). **b.** Maximum normalized RFU measurements (black) and respective apparent reaction rates (red) of FLARE reactions requiring either dATP, dGTP or dCTP production. Reduction of different endogenous NDPs resulted in similar reaction rates, around 50-60% of the positive control signal. **c.** Maximum normalized RFU measurements (black) and respective apparent reaction rates (red). of FLARE reactions lacking either dTTP or all dNTPs, both with rates reaching about 15% of positive control signal, but significantly higher than the negative control (dTTP-limiting vs negative control, p=0.0064) (dNTP-limiting vs negative control, p=0.0064). The data was normalized with min-max scaling between max value of the ΔRNR-dNTPs sample and t0 of the ΔRNR-dDTPs sample. Technical replicates were performed for all measurements, with n = 3. The mean and standard deviation are shown. Unpaired two-tailed Welch's t-tests were used for pairwise comparisons between the different reaction rates out and corrected for multiple comparisons with FDR.

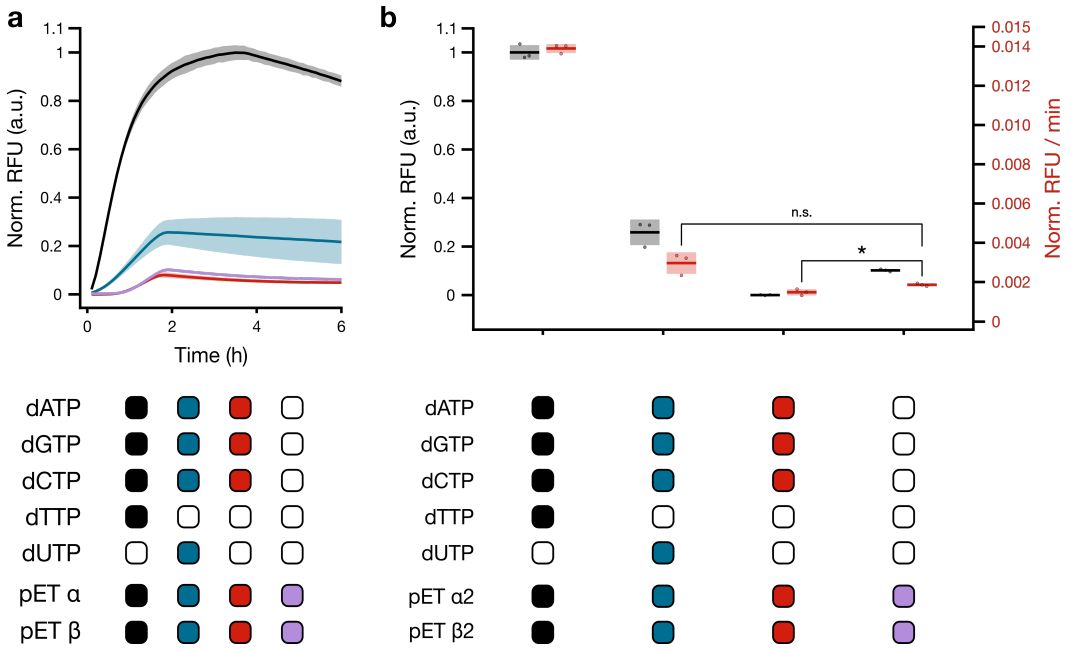

Supplementary Figure 9: Incorporation of dUTP in FLARE assay in PURE.

Testing dUTP concentration dependency of FLARE assay read-out. In the sample matrices, colored boxes indicate components supplied to the reactions. **a.** Normalized real-time RFU measurements. Samples containing 200 µM dVTPs (dATP, dGTP, dCTP) were supplied with either 200 µM dTTP (black), 200 µM dUTP (blue) or no dTTP or dUTP (red). Alternatively, samples lacked dNTPs entirely (purple). **b.** Maximum normalized RFU values (black), compared with their respective observed apparent rates (red). The ΔdNTPs sample was compared to the dVTPs ($p=0.0446$) and dVTPs + dUTP samples ($p=0.0707$). While a higher RFU signal is achieved when 200 µM of additional dUTP are supplied to the system, the reaction rates remain similar to the samples lacking dTTP or dUTP, albeit these show a longer signal delay. The data was normalized with min-max scaling between maximum value and t0 of the samples with dATP, dGTP, dCTP, dTTP. Technical replicates were performed for all measurements, with n = 3. The mean and standard deviation are shown. Unpaired two-tailed Welch's t-tests were used for pairwise comparisons between the different reaction rates out and corrected for multiple comparisons with FDR.

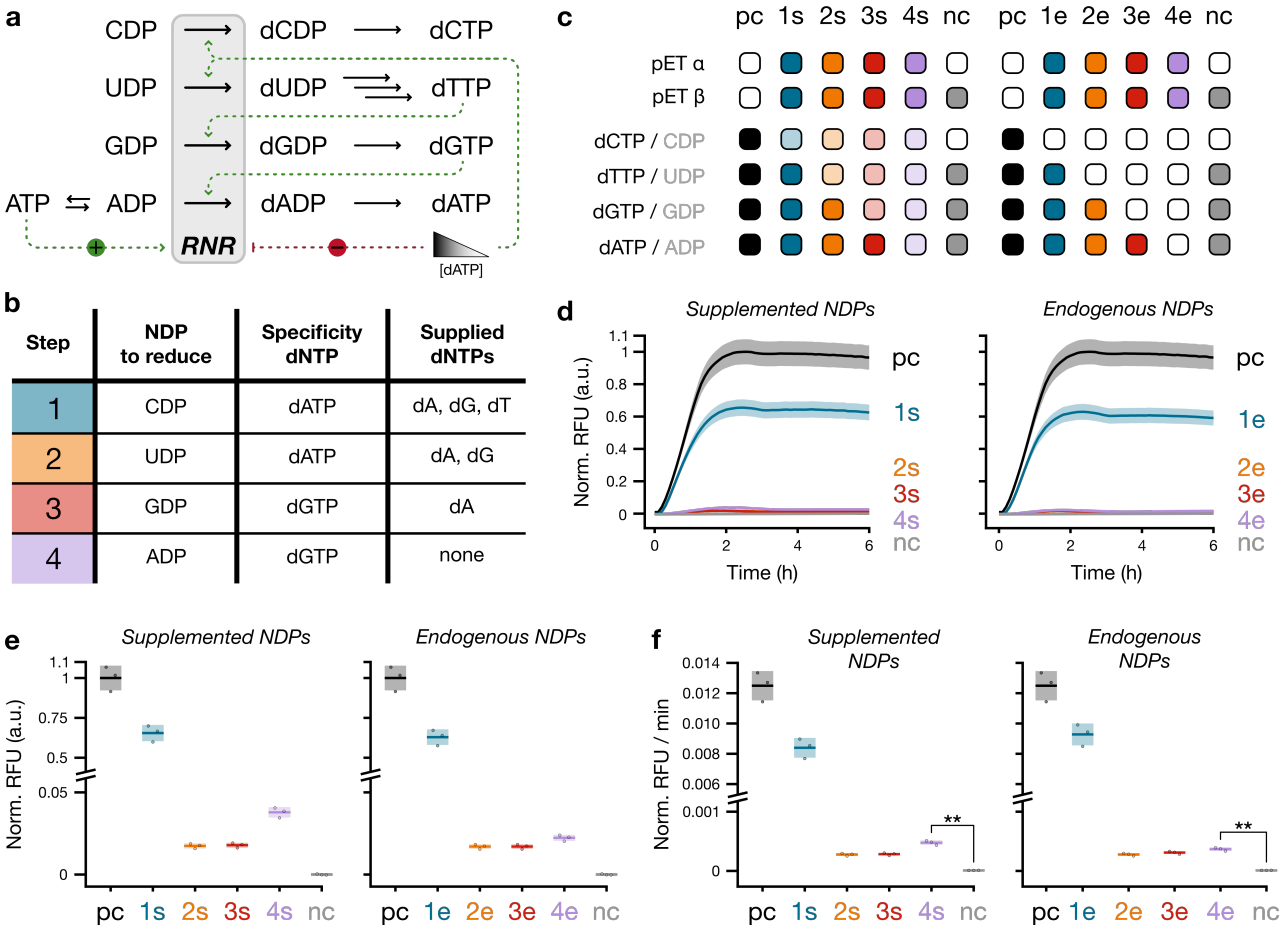

Supplementary Figure 10: Simulation of RNR Ia allosteric regulation with de novo expressed RNR Ia.
Stepwise replacement of dNTPs supplied to FLARE reactions with NDPs (either supplemented to PURE or endogenously produced in PURE) to recreate the allosteric regulatory pattern of RNR Ia reconstructed from mechanistic studies.[8,9] **a.** Regulatory pattern of RNR Ia. Allosteric regulations that activate reduction of specific NDPs are highlighted in green, while regulations that inhibit RNR Ia activity are highlighted in red. ATP acts as the general activity effector, while increasing concentrations of dATP inhibit RNR Ia activity. The gray triangle represents the changing concentrations of dATP. Low dATP concentrations at the beginning of the cascade act as the specificity effector for dCTP and dUTP synthesis, while high dATP concentrations inhibit RNR Ia activity. dTTP is the specificity effector for dGTP, which is in turn the specificity effector for dATP synthesis. **b.** The allosteric regulation is broken down in "steps" for simulation with FLARE, each of which represents a combination of specificity effector and substrate, which, when reduced, acts as the next specificity effector. For each NDP to be reduced, enough of the corresponding specificity dNTP needs to be generated in the previous step. **c.** Sample matrix, where colored boxes represent components added to the reactions. “pc” and “nc” represent positive (i.e. ΔRNR-dNTPs) and negative (i.e. ΔRNR-dDTPs) controls, respectively. Shaded boxes represent respective NDPs supplied to the reactions on top of standard PURExpress composition. **d.** Normalized real-time RFU measurements with different NDP/dNTP combinations for each step in the reaction cascade. **e.** Maximum RFU values from FLARE reactions. **f.** Apparent reaction rates of FLARE reactions. As seen previously, samples lacking dNTPs generated stronger signals and faster kinetics compared to the ΔRNR-dDTPs negative control, either with NDPs supplemented ($p=0.0029$) or with NDPs supplied by PURE's machinery ($p=0.0029$). The data was normalized with min-max scaling between maximum value of the ΔRNR-dNTPs sample and t0 of the ΔRNR-dDTPs sample. Technical replicates were performed for all measurements, with $n = 3$. The mean and standard deviation are shown. Unpaired two-tailed Welch’s t-tests were used for pairwise comparisons between the different reaction rates out and corrected for multiple comparisons with FDR.

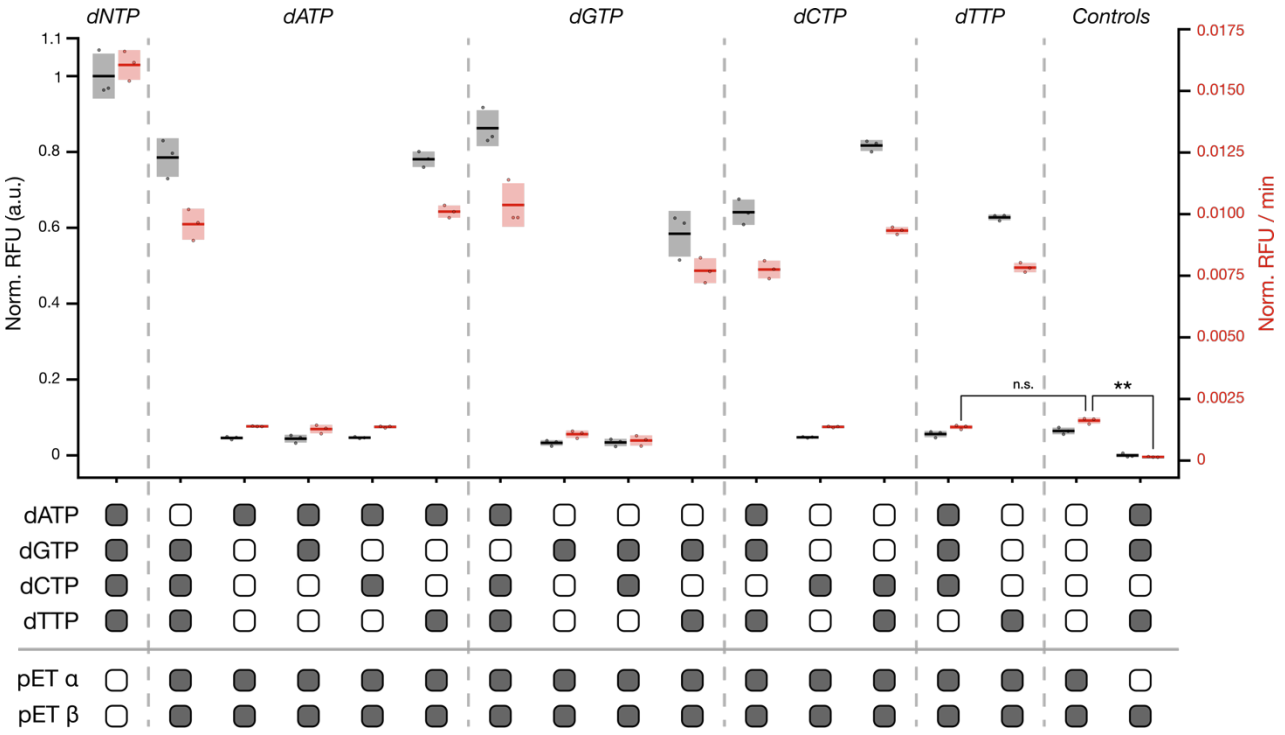

Supplementary Figure 11: FLARE assay in PURExpress with all dNTP combinations.

Screening of all 16 possible combinations of dNTPs input to determine effect on regulatory mechanism by input dNTP content. Shown here, maximum normalized RFU values (black) of combinations of dNTPs supplied to FLARE reactions, compared with their respective observed apparent rates (red). In the sample matrix, dark gray boxes indicate components supplied to the reactions. FLARE apparent rates clustered between around 50-60% of the positive control's rate, apart from when dTTP needs to be synthesized in PURE from UDP. In these cases, signals reached about 10% of the positive control, resulted similar to the rates of the sample dependent on reduction of all endogenous NDPs (dVTPs vs ΔdNTPs, p=0.054) and were significantly higher than the negative control (ΔdNTPs vs ΔpETα-dDTPs, p=0.003). Data is normalized with min-max scaling between max value of the ΔRNR-dNTPs sample and t0 of the ΔpET α-dDTPs sample. Technical replicates were performed for all measurements, with n = 3. The mean and standard deviation are shown. Unpaired two-tailed Welch's t-tests were used for pairwise comparisons between the different reaction rates out and corrected for multiple comparisons with FDR.

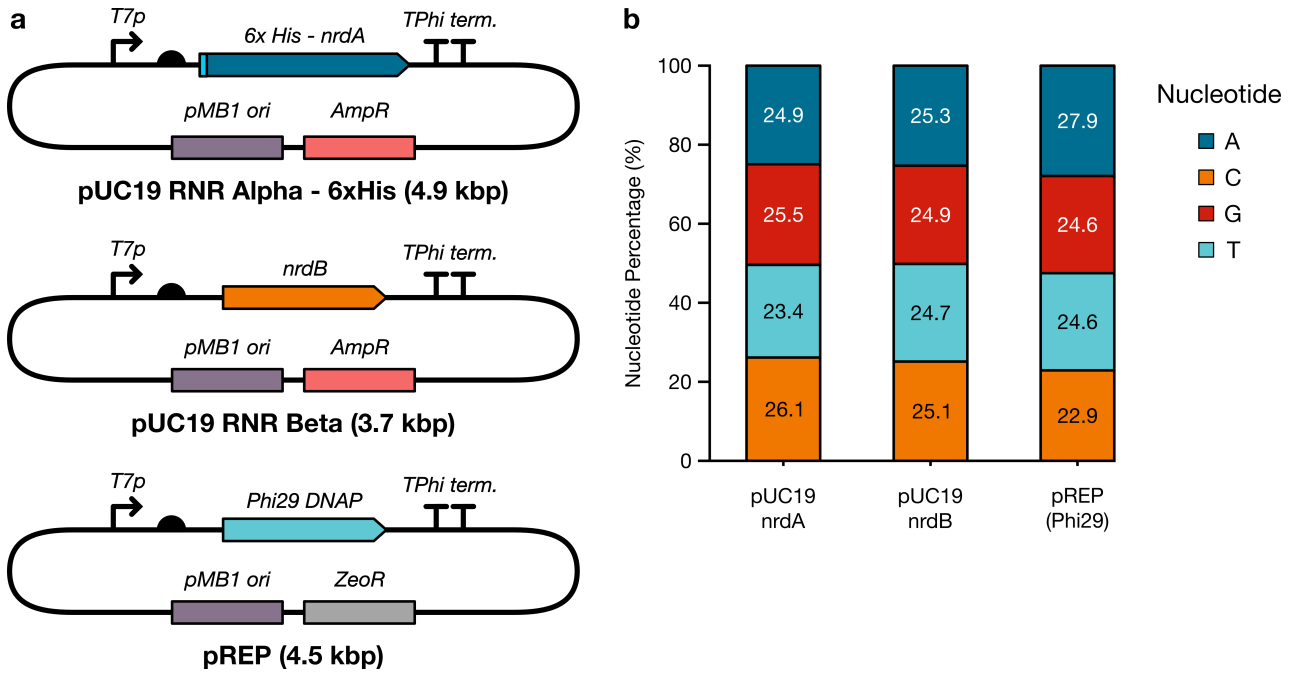

Supplementary Figure 12: Maps of pUC19 RNR Ia plasmids and pREP (Phi29 DNAP) plasmid.

a. Schematic maps of pUC19 plasmids encoding individual RNR subunits (*nrdA* - Alpha, *nrdB* - Beta) and pREP, encoding for Phi29 DNA polymerase. All RNR plasmids are constructed with the identical T7 promoter, ribosome binding site and double TPhi terminator. pREP was constructed for optimized expression in TTcDR PURE.[10] **b.** Percentage of each nucleotide in the pUC19 RNR plasmids and in pREP.

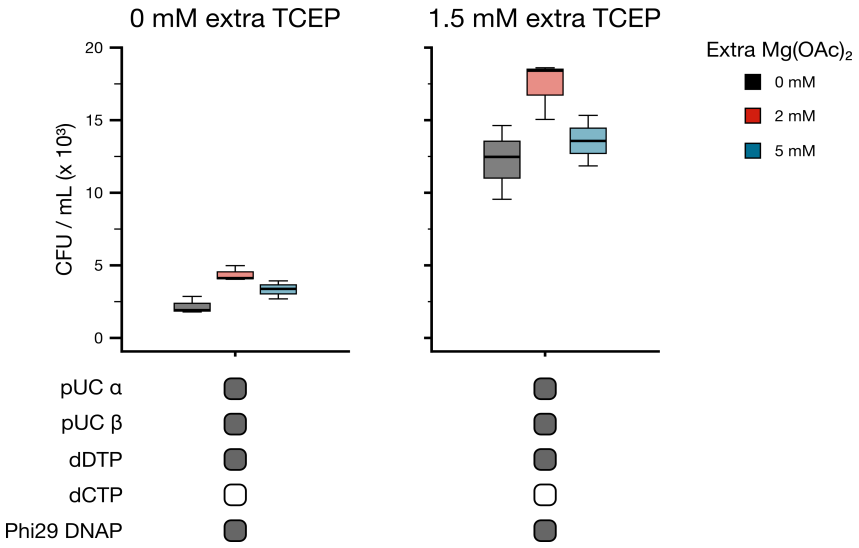

Supplementary Figure 13: Transformation efficiencies of replication products after TTcDR and circle-to-circle ligation in presence or absence of additional TCEP and at different $Mg(OAc)_2$ concentrations.

Different concentrations of TCEP and $Mg(OAc)_2$ were tested for their effects on transformation efficiency of TTcDR products independent on RNR Ia activity. TTcDR reactions were prepared as described above. Either no extra TCEP or 1.5 mM extra TCEP was supplied to reactions. For each TCEP condition, either 0, 2 or 5 mM of extra $Mg(OAc)_2$ were supplied to the reactions. TTcDR reactions were then incubated at 30 ºC for 16 hours and then treated for C2C re-circularization of TTcDR products prior to transformation with in house-produced electrocompetent *E. coli* MegaX cells and plated on LB agar with 100 µg/mL carbenicillin. Technical replicates were performed for all measurements, with n = 3. The median, standard deviation and 95% confidence interval are shown.

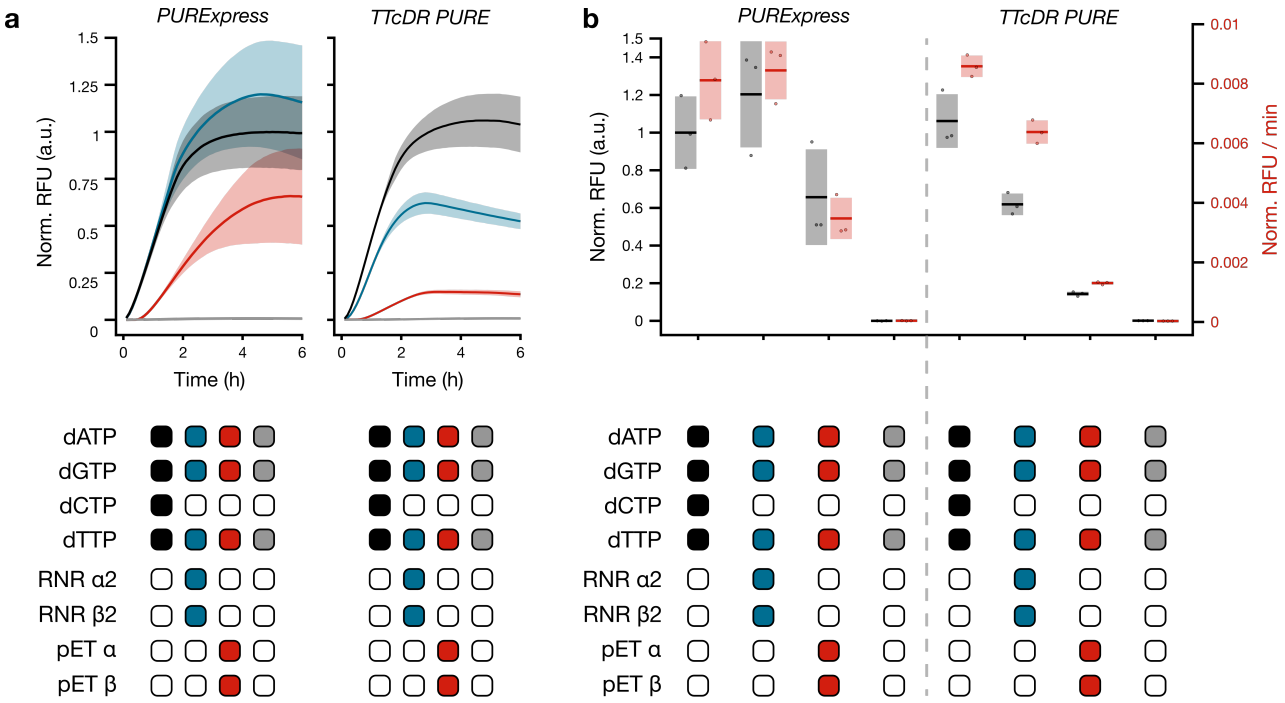

Supplementary Figure 14: FLARE activity in PURExpress and TTcDR PURE with either purified or de novo RNR Ia.

Comparison of FLARE assay read-out in PURExpress or TTcDR PURE. In both cases, read-out is dependent on either purified RNR Ia subunits, or de novo expressed RNR Ia. In the sample matrices, colored boxes indicate components supplied to the reactions. RNR-independent read-outs (black boxes) were compared with read-outs dependent on dCTP synthesis by either purified RNR Ia (blue boxes) or de novo RNR Ia (red boxes) in different PURE systems. The negative control without RNR Ia and only dDTPs supplemented to the reactions is represented by gray boxes. **a.** Normalized real-time RFU measurements comparing FLARE between the two PURE systems. **b.** Maximum normalized RFU values (black), compared with their respective observed apparent rates (red). The data is normalized with min-max scaling between max value of the ΔRNR-dNTPs sample and t0 of the ΔRNR-dDTPs sample of PURExpress. Independent replicates were performed for all measurements, with n = 3. The mean and standard deviation are shown.

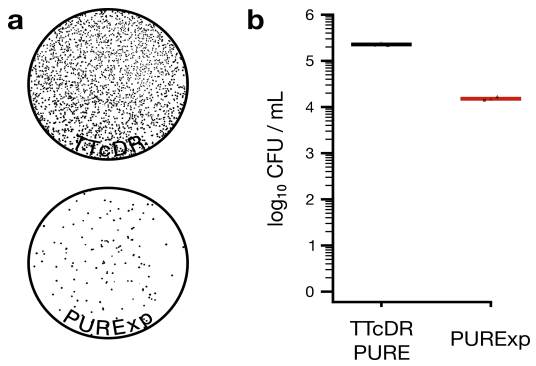

Supplementary Figure 15: Transformation efficiency with TTcDR PURE and PURExpress.

Comparing transformation efficiency of pUC19 after DNA replication in either TTcDR PURE or PURExpress. 3 nM of pUC19 were replicated for 16 hours at 30 ºC in either TTcDR PURE (optimized for RNR Ia) or PURExpress, treated with 60 U of DpnI and then transformed in electrocompetent *E. coli* MegaX cells (prepared in house). **a.** Example plate images, shown as binary images after thresholding. **b.** Colony-forming unit count per mL of recovery culture (CFU/mL) count of pUC19 replicated in either TTcDR PURE or PURExpress. Technical replicates were performed for all measurements, with n = 3. The mean and standard deviation are shown.

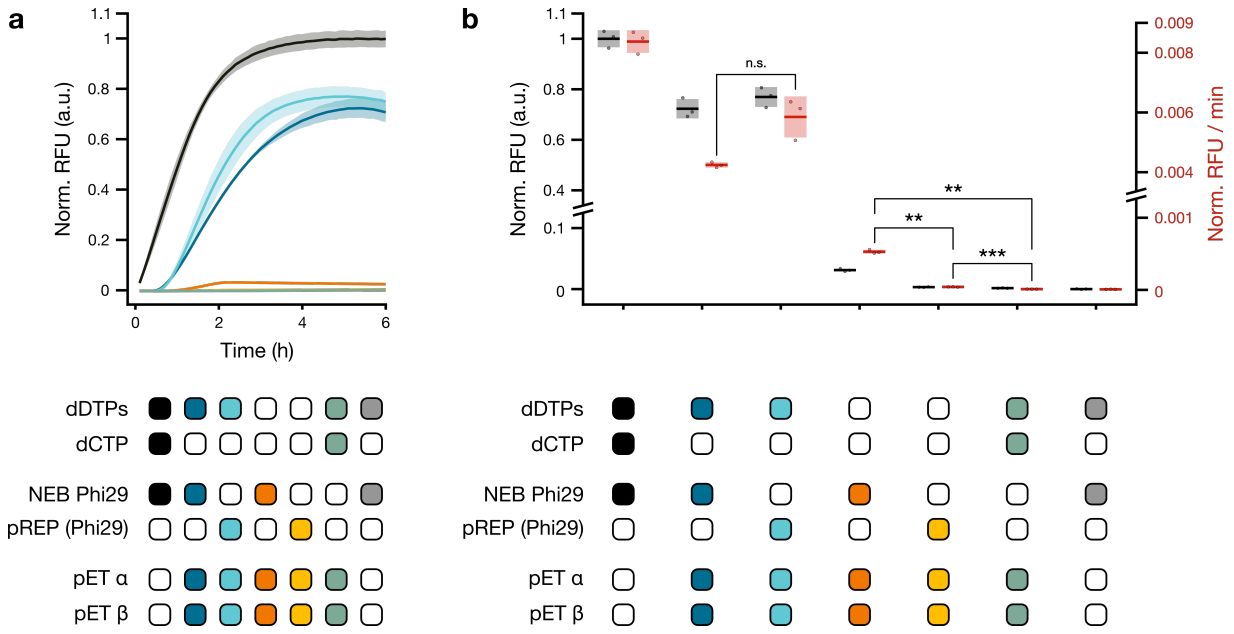

Supplementary Figure 16: FLARE assay comparing supplied purified Phi29 DNAP and de novo Phi29 DNAP.

FLARE assay with de novo RNR Ia, comparing read-outs with Phi29 DNAP either purified (10 U, NEB) or expressed de novo from pREP plasmid. In the sample matrices, colored boxes indicate components supplied to the reactions. Positive control (black) without RNR Ia, with all dNTPs supplied and purified Phi29 DNAP. Negative controls with all dNTPs, but lacking Phi29 DNAP (green), or without RNR Ia, with purified Phi29 DNAP and only dDTPs. These samples are compared to samples that depend on RNR Ia and Phi29 DNAP synthesis: dCTP synthesis (purified Phi29 DNAP - dark blue; expressed Phi29 DNAP - light blue) or full dNTPs synthesis (supplied Phi29 DNAP - dark orange; expressed Phi29 DNAP - light orange). **a.** Normalized real-time RFU measurements. **b.** Maximum normalized RFU values (black), compared with their respective observed apparent rates (red). Reaction rates with dCTP synthesis are comparable between supplied and expressed Phi29 DNAP (p=0.0564), but rates of dNTP synthesis read-out with purified Phi29 DNAP are higher compared to expressed Phi29 DNAP (p=0.0015). However, in both cases, reaction rates of dNTP synthesis are higher than when no Phi29 DNAP was present in the system (compared to purified Phi29 DNAP, p=0.0015; compared to expressed Phi29 DNAP, p=0.0010). The data was normalized with min-max scaling between max value of the ΔRNR-dNTPs sample and t0 of the ΔRNR-dDTPs sample. Technical replicates were performed for all measurements, with n = 3. The mean and standard deviation are shown. Unpaired two-tailed Welch's t-tests were used for pairwise comparisons between the different reaction rates out and corrected for multiple comparisons with FDR.

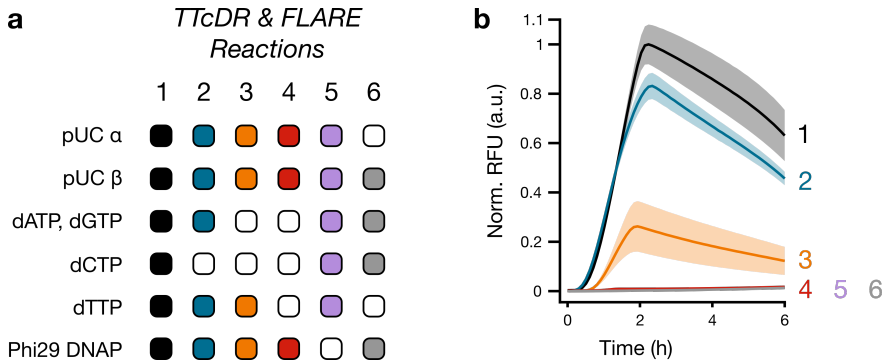

Supplementary Figure 17: Detection of coupled reduction of multiple endogenous NDPs by de novo RNR Ia, with generation of dsDNA template by de novo Phi29 DNAP.

FLARE read-out dependent on de novo expression of the minimal DNA biosynthesis and replication system (i.e. RNR Ia and Phi29 DNAP), combined with detection of reduction of different dNTP combinations supplied to PURE. **a.** Reaction matrix for the characterization of DNA synthesis and replication dependent on RNR Ia and Phi29 DNAP. Colored boxes indicate components added to the reactions. RNR-independent DNA replication with all dNTPs supplied (black) is compared to RNR-dependent reduction of endogenous CDP (blue), endogenous VDP (i.e. ADP, GDP, CDP) (orange), endogenous NDPs (red). Negative controls: dNTPs and ΔPhi29 (purple) and dDTPs and Δα (grey). **b.** Normalized real-time RFU measurements. Fluorescence was detected when dCTP and dVTPs (i.e. dATP, dGTP and dCTP) were synthesized, but not when all dNTPs were produced. This is possibly due to lower Phi29 DNA polymerase expression. The data was normalized with min-max scaling between max value of the sample with all dNTPs and t0 of the ΔpETα-dDTPs sample. Technical replicates were performed for all measurements, with n = 3. The mean and standard deviation are shown.

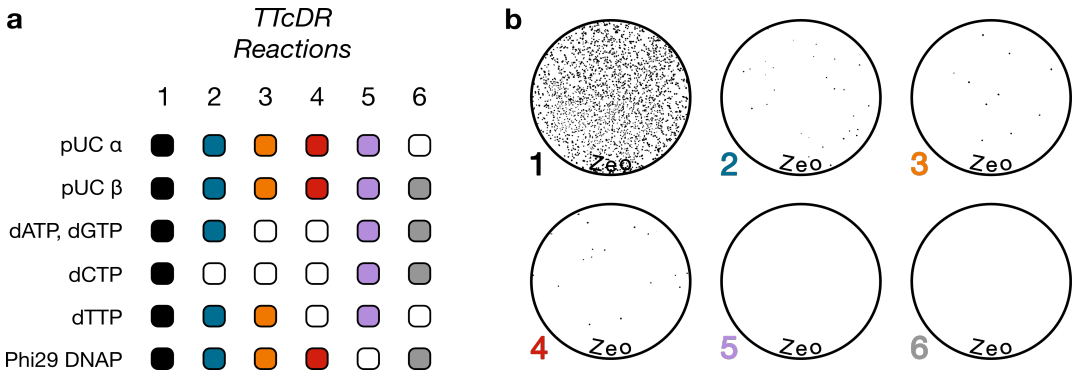

Supplementary Figure 18: Transformation of TTcDR products dependent on RNR Ia and pREP.

Transformation of TTcDR products was confirmed by plating on plates containing either carbenicillin (for pUC RNR plasmids - shown in main text) or zeocine (for pREP) (see main text Fig. 5). **a.** Sample matrix. Colored boxes represent the components included in the reaction. **b.** Example images of LB agar plates with zeocine resistance marker for selection of transformants with pREP plasmid, shown as binary images after thresholding. TTcDR reactions were carried out in independent replicates (n=3) and each replicate was transformed three times. Total number of transformations for each sample n=9. A single example of a transformation is shown for each sample.

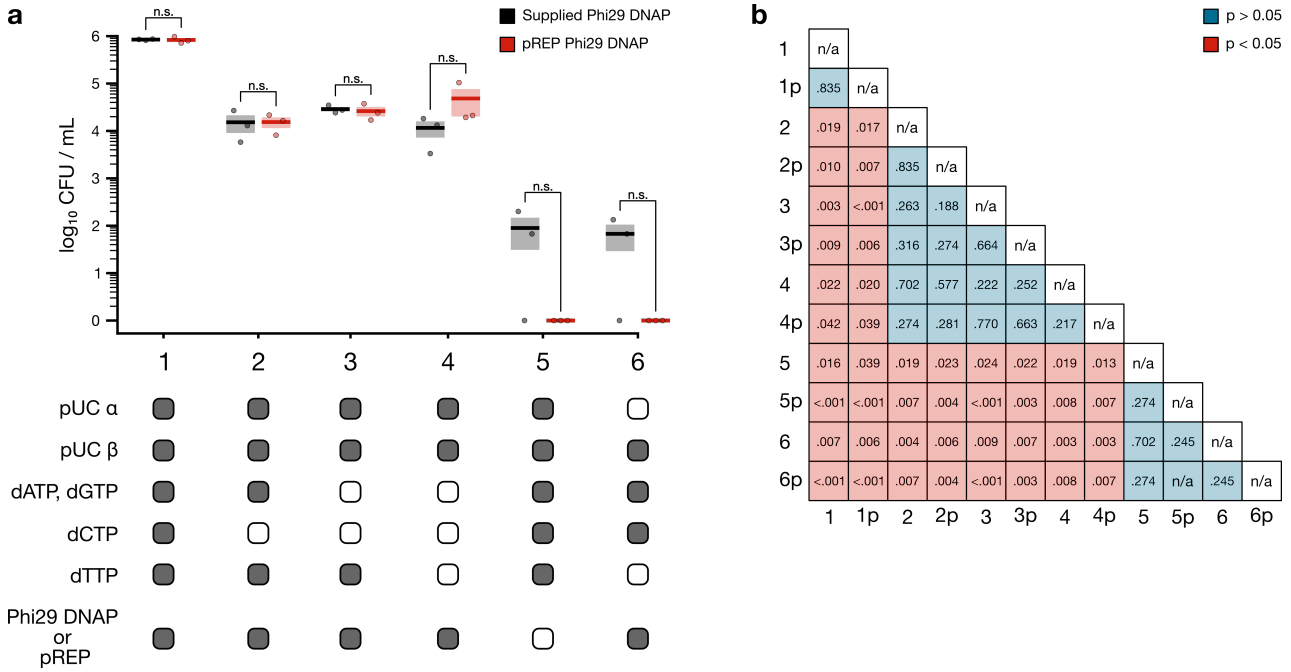

Supplementary Figure 19: Comparison of CFU count from TTcDR reactions with either supplied or expressed Phi29 DNAP.

Transformation of TTcDR products generated by de novo RNR Ia and Phi29 DNAP either supplied or expressed in PURE. 1 µL of 1:10 dilution of all TTcDR reactions were transformed in commercial electrocompetent *E. coli* MegaX. Data shown here is collated from Fig. 4c, 5d and 5e from main text to compare reactions depending on their source of Phi29 DNAP. **a.** Colony-forming unit count per mL of recovery culture (CFU/mL) comparison from reactions with Phi29 DNAP either supplied (black) or expressed de novo (red). The reaction matrix specifies the content of each reaction. Independent reaction replicates n = 3. Each replicate is transformed 3 times. Overall mean of n = 9 and SEM of individual replicate means are shown, along with means of individual replicates. **b.** p values of pairwise Welch's two-tailed unpaired t-test pairwise comparisons across all samples. Sample composition and numbering are the same as shown in **a.** and "*p*" indicates pREP as source for Phi29 DNAP. All p values presented here are corrected for multiple comparisons with the Benjamini-Hochberg procedure (i.e. FDR). The p values less than the 0.05 alpha value for FDR are shown in red and the ones above 0.05 in blue. This comparison highlights that regardless of the type of input of Phi29 DNAP, reactions with the same dNTP content are comparable with each other. Furthermore, all RNR-dependent reactions are comparable with each other, irrespective of Phi29 DNAP input or dNTP synthesis requirements.

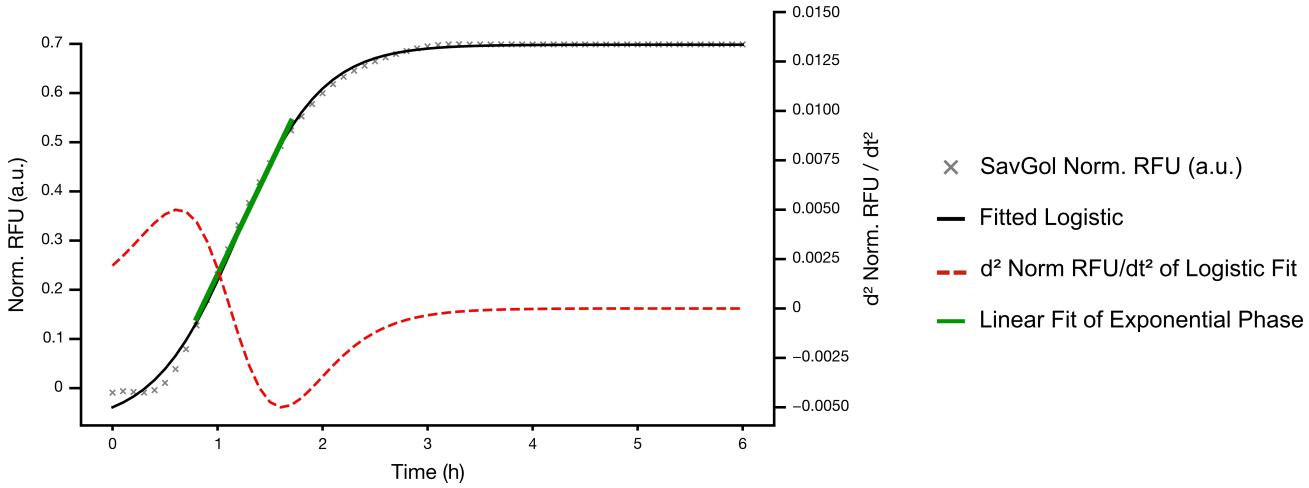

Supplementary Figure 20: Example image of FLARE apparent rate estimation.

A single replicate of a reaction for the reduction of endogenous CDP by de novo expressed RNR Ia (i.e. pET α, pET β and dDTPs) is shown here. (i.e. pET α, pET β, dDTPs). Min-max normalized RFU data was smoothened using a Savitzky-Golay filter (gray crosses). The data was fit to a scaled logistic function (black) and the second derivative was computed (red). The local maximum and minimum of the second derivative were used to define the *x*-coordinates between which a linear regression model of the smoothed data is fit (green). The apparent rate of a FLARE reaction is then defined as the slope of the computed linear model.

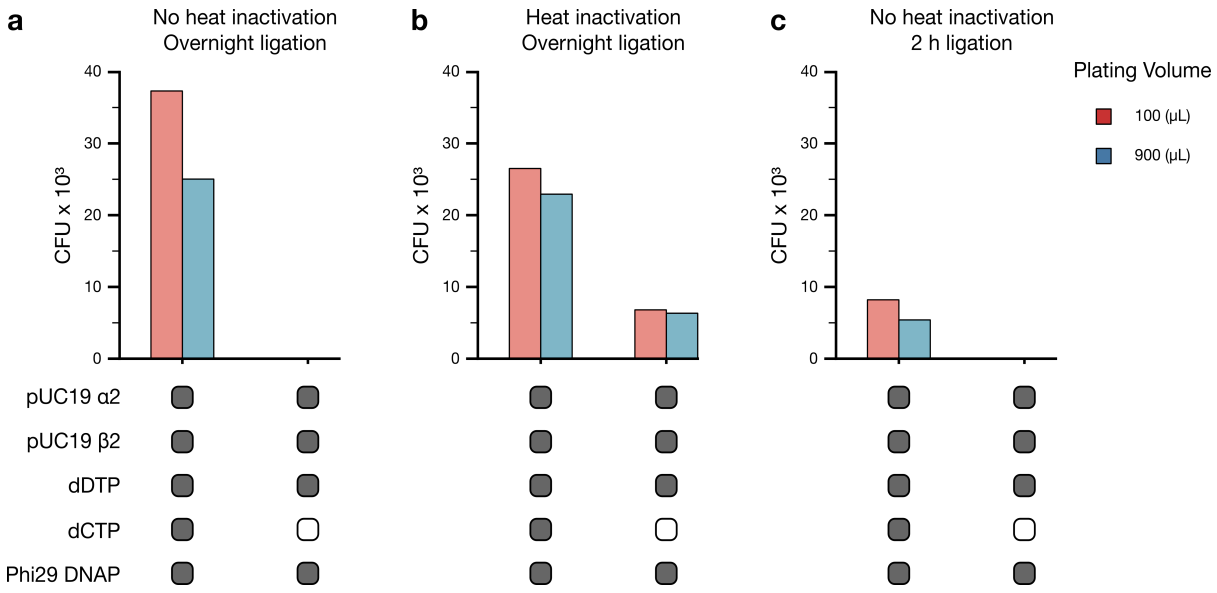

Supplementary Figure 21: Transformation efficiency of TTcDR products with C2C protocol variations.

TTcDR reactions were prepared as previously described and incubated at 30 ºC for 16 hours. RNR-independent DNA replication (i.e. with dNTPs) was compared with RNR-dependent replication (i.e. with dDTPs). TTcDR products were transformed in in house-produced electrocompetent *E. coli* MegaX. **a.** CFU count of TTcDR sample without heat-inactivation after restriction digest and with overnight ligation by Salt-T4 DNA ligase. **b.** CFU count of TTcDR sample with 20 minutes heat-inactivation at 85 ºC after restriction digest, followed by overnight ligation by Salt-T4 DNA ligase. **c.** CFU count of TTcDR sample without heat-inactivation after restriction digest and with 2-hour ligation by Salt-T4 DNA ligase. n=1, each sample was plated twice.

Supplementary References

1. Yokoyama, K., Uhlin, U. & Stubbe, J. Site-Specific Incorporation of 3-Nitrotyrosine as a Probe of pKa Perturbation of Redox-Active Tyrosines in Ribonucleotide Reductase. *J. Am. Chem. Soc.* **132**, 8385–8397 (2010).

2. Nick, T. U., Ravichandran, K. R., Stubbe, J., Kasanmascheff, M. & Bennati, M. Spectroscopic Evidence for a H Bond Network at Y356 Located at the Subunit Interface of Active E. coli Ribonucleotide Reductase. *Biochemistry* **56**, 3647–3656 (2017).

3. Pagba, C. V. *et al.* A tyrosine–tryptophan dyad and radical-based charge transfer in a ribonucleotide reductase-inspired maquette. *Nat. Commun.* **6**, 30 (2015).

4. Lin, Q. *et al.* Glutamate 52-β at the α/β subunit interface of Escherichia coli class Ia ribonucleotide reductase is essential for conformational gating of radical transfer. *J. Biol. Chem.* **292**, 9229–9239 (2017).

5. Cui, C. *et al.* Gated Proton Release during Radical Transfer at the Subunit Interface of Ribonucleotide Reductase. *J. Am. Chem. Soc.* **143**, 176–183 (2021).

6. Kasanmascheff, M., Lee, W., Nick, T. U., Stubbe, J. & Bennati, M. Radical transfer in E. coli ribonucleotide reductase: a NH2Y731/R411A-α mutant unmasks a new conformation of the pathway residue 731. *Chem. Sci.* **7**, 2170–2178 (2016).

7. Lee, W. Mechanistic Studies of the Radical Transport Pathway in Aminotyrosine-Substituted Class Ia Ribonucleotide Reductase. (Massachussets Institute of Technology, Boston, MA, USA, 2018)

8. Zimanyi, C. M., Chen, P. Y., Kang, G., Funk, M. A. & Drennan, C. L. Molecular basis for allosteric specificity regulation in class Ia ribonucleotide reductase from Escherichia coli. *eLife* **5**, e07141 (2016).

9. Cooperman, B. S. & Kashlan, O. B. A comprehensive model for the allosteric regulation of Class Ia ribonucleotide reductases. *Adv. Enzyme Regul.* **43**, 167–182 (2003).

10. Libicher, K., Hornberger, R., Heymann, M. & Mutschler, H. In vitro self-replication and multicistronic expression of large synthetic genomes. *Nat. Commun.* **11**, 904 (2020).